CO$_2$ as an oxidant for high-temperature reactions

Sibudjing Kawi * and Yasotha Kathiraser

Department of Chemical and Biomolecular Engineering, Faculty of Engineering, National University of Singapore, Singapore, Singapore

This paper presents a review on the developments in catalyst technology for the reactions utilizing CO$_2$ for high-temperature applications. These include dehydrogenation of alkanes to olefins, the dehydrogenation of ethylbenzene to styrene, and finally CO$_2$ reforming of hydrocarbon feedstock (i.e., methane) and alcohols. Aspects on the various reaction pathways are also highlighted. The literature on the role of promoters and catalyst development is critically evaluated. Most of the reactions discussed in this review are exploited in industries and related to on-going processes, thus providing extensive data from literature. However, some reactions, such as CO$_2$ reforming of ethanol and glycerol, which have not reached industrial scale, are also reviewed owing to their great potential in terms of sustainability, which is essential as energy for the future. This review further illustrates the building-up of knowledge that shows the role of support and catalysts for each reaction and the underlying linkage between certain catalysts, which can be adapted for the multiple CO$_2$-related reactions.

Keywords: CO$_2$ utilization, reforming, dehydrogenation, catalyst, hydrocarbon

INTRODUCTION

Rising levels of CO$_2$ in atmosphere caused severe impacts, such as the increasing intensities of hurricanes, influence of El Nino phenomena, reduced calcification of marine plankton, and deglaciation (Wu and Kawi, 2009). It is clear that it is important to stabilize CO$_2$ levels to prevent escalation, but it is even more ideal to reduce CO$_2$ concentrations in order to avoid catastrophic and irreversible environmental damage (Styring and Armstrong, 2011). Presently, a major practice of abating CO$_2$ emission involves capture and storage technologies whereby CO$_2$ will remain in supercritical conditions during storage (Styring and Armstrong, 2011). Nevertheless, the transportation of CO$_2$ through pipelines is carried out under liquid conditions (McCoy and Rubin, 2008) and injection of CO$_2$ is carried out in liquid form as well (Vilarrasa et al., 2013); therefore, from this aspect there is no safety issue. This, however, overlooks the fact that, besides depletion of storage space, for every molecule of CO$_2$ stored; there is one less carbon atom participation in the carbon economy. Chemical utilization of CO$_2$, being one of the major greenhouse gases, is an important step toward a mature technology that contributes to C–C cycling and reduction in CO$_2$ concentrations, as well as toward economic, renewable, and environmental synthesis of value added product (Ansari and Park, 2012; Aresta et al., 2013).

One of the major concerns regarding CO$_2$ chemical utilization is related to the thermodynamic stability of the CO$_2$ molecule. Additional energy and co-reactants are required for full conversion of the CO$_2$ molecule into value-added products. However, recent improvement in efficiency of sustainable energy supplies, such as solar and geothermal, enhances the economical viability of CO$_2$ utilization. One of the technologies that are gaining prominence is the utilization of CO$_2$ as an oxidant for catalytic transformations under dehydrogenation as well as reforming reactions under high-temperature environments. The main highlight of this review is to focus on the utilization of CO$_2$ as an oxidant for alkane dehydrogenation as well as reforming of hydrocarbons to synthesis gas, which is the building block for chemical synthesis.

According to Bartholomew (1984), the oxidizing ability of various gases in carbon gasification is in the order of O$_2$ (105) > H$_2$O (3) > CO$_2$ (1) > H$_2$ (0.003). Among these gases, O$_2$ is widely used for oxidative dehydrogenation (ODH) reactions, whereas water in the form of steam is used for reforming of hydrocarbon/alcohol reactions.

OXIDATIVE DEHYDROGENATION OF ALKANES

CO$_2$ utilization in the ODH of alkanes has received significant attention in recent years. By co-feeding CO$_2$ in the ODH of light alkanes, as a "soft oxidant," the reaction equilibrium is shifted toward more olefin production (Urlan et al., 2008; Raju et al., 2014). The ODH reaction is interesting as it can directly produce olefins, such as ethylene, propylene, and butylenes, from their respective alkane sources. These olefins are known to be building blocks in the petrochemical industry. For example, ethylene is widely used for the production of plastics, polymers, fibers, and packaging materials (Qiao et al., 2014). The industrial synthesis of ethylene via steam cracking of hydrocarbons or naphtha is very energy consuming, and the catalysts are afflicted by coking resulting in catalyst deactivation (Qiao et al., 2014). Therefore, it is more desirable to utilize an oxidant capable of mildly oxidizing the reaction environment in order to inhibit the coking phenomenon. Usage of molecular oxygen as oxidant can effectively reduce the reaction temperature and inhibit coking, however, issues such as low selectivity due to the production of CO$_x$ species from HCs and the need to remove excess heat of reaction prevail (Rangel et al., 2012). However, CO$_2$ has been found to serve as a suitable medium for heat supply for the endothermic dehydrogenation reaction and as a coke removal agent from the catalyst (Urlan et al., 2008). In

addition, CO$_2$ improves olefin selectivity compared to molecular O$_2$ by preventing deep oxidation of the reaction products, thus improving the olefin selectivity (Liu et al., 2011).

The general reaction pathway for the CO$_2$-ODH is shown in Eq. 2.1:

$$C_nH_{n+2} + CO_2 \rightarrow C_nH_n + CO + H_2O \qquad (2.1)$$
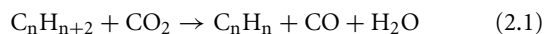
It should be noted that the olefins produced from dehydrogenation of higher alkanes, contain allylic hydrogens, which are coke precursors, being the main cause of catalyst deactivation, which in turn leads to low olefin yields. Thus, optimization of catalyst systems is of paramount importance for this process. On the other hand, the CO and H$_2$O by-products can be reacted together for the production of hydrogen via the low-temperature water gas shift reaction. However, pure CO, by itself has many uses in the chemical industry especially as a secondary feedstock for production of acetic acid by methanol carbonylation process, production of phosgene, formic acid, etc.

The patented processes for ODH of hydrocarbons are usually based on the concept of utilizing oxidants, such as O$_2$, CO$_2$ and SO$_2$, coupled with steam in order to shift the equilibrium of the dehydrogenation reaction toward enhanced conversion. Steam was used to activate the catalyst as well as function as a coke removal agent via the water gas shift reaction in an invention described by Budin and Meyer (2003). More recently, Smith (2008) described a process in which ethane and ethylbenzene are simultaneously dehydrogenated in the presence of CO$_2$ or steam at temperatures ranging between 500 and 700°C in the presence of catalysts comprising transition metals (V, Cr, Mn, Fe, Co, Ni, etc.) and supported on high surface area supports. This method results in the production of a mixed product feed stream comprising ethylene, styrene, ethylbenzene, ethane, hydrogen, water, CO, and CO$_2$, whereby the ethane and ethylene product stream can be recycled in other processes, which include alkylation of benzene or other polymerization processes.

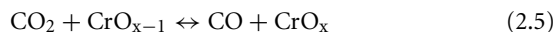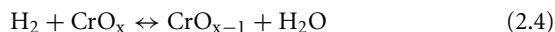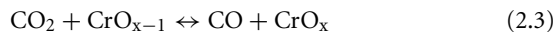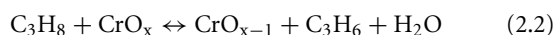## CATALYTIC SYSTEMS FOR CO$_2$-ODH OF ALKANES

It should be noted that catalysts with redox properties, such as molybdenum-, chromium- and vanadia-based catalysts, possess high catalytic activity for the various ODH reactions of hydrocarbons (Solymosi et al., 2001; Michorczyk et al., 2012). The main factors influencing the reaction include acid–base bifunctionality, which is important in CO$_2$-mediated dehydrogenation reactions since both basic sites and Lewis-acid vacant sites play important functions in hydrocarbons activation (Deng et al., 2007; Pramod et al., 2014).

Investigations on chromium-based catalysts supported on mixed oxides, mesoporous silica, and zeolites (Zhang et al., 2002; Takehira et al., 2004; Zhao and Wang, 2006) have been carried out for CO$_2$-ODH (Nakagawa et al., 2003). These supports possess high surface area that ensures good catalyst dispersion, which is essential for high catalytic activity and stability. Cr-based catalysts supported on zeolitic TS-1 (Zhang et al., 2002), high silica H-ZSM-5 (Mimura et al., 2006), and siliceous MCM-41 (Takehira et al., 2004) were shown to exhibit good activity and selectivity for the CO$_2$-ODH reaction of ethane and propane. However, in spite

of their high catalytic activity, reduction of the active chromium species led to catalyst deactivation. According to Takehira et al. (2004), based on EXAFS data, the coordinatively unsaturated tetrahedral Cr(VI) represents the active site for alkane dehydrogenation; whereas the coordinatively saturated bulk Cr(III) ions are less active for alkane dehydrogenation (Cavani et al., 1996; Liu et al., 2007). CO$_2$ plays an important role in regenerating the deactivated catalyst. Similar to mesoporous-based supports, the catalytic activity of chromium supported on silica was found to depend on the chromium dispersion (Botavina et al., 2008). Based on the study by Botavina et al. (2008), DR-UV–vis studies indicate that surface chromates with lower nuclearity possess high activity compared to Cr(VI) in the form of extended polychromates (less dispersed).

Besides supporting catalysts on the mesoporous supports, it is also possible to incorporate the catalyst within mesoporous structures. For example, Liu and Li (2006) synthesized Cr incorporated into MSU-1 (a type of mesoporous molecular sieve) and Cr supported on MSU-1, the former labeled as Cr-MSU-1 and the latter as Cr/MSU-1 for CO$_2$-ODH of ethane. They found that despite higher activity for the Cr supported catalysts, especially at Cr loading >1 wt%, however, it also resulted in lower selectivity due to cracking reactions caused by a higher ratio of inactive polychromate species. Furthermore, the catalyst dispersion at higher than 8 wt% loading is severely affected resulting in the decrease of Cr(VI) species and increase in crystallite Cr$_2$O$_3$ species (Liu et al., 2007). Recently, Baek et al. (2012) synthesized highly dispersed chromium oxide catalysts supported on mesoporous silica using an electrostatically controlled assembly process. A high (90%) selectivity toward propylene formation was achieved with a yield of 30% in the CO$_2$-ODH of propane. Within 25 h, propane conversion reached steady state and the deactivation observed was related to coke formation and reduction of active chromium sites.

CO$_2$ as oxidant (**Scheme 1**) enhances regeneration of the reduced chromium sites formed during the dehydrogenation of propane (Eq. 2.2) and the successive reduction with H$_2$ (Eq. 2.3) (Michorczyk et al., 2012), where CrO$_x$ represents the oxidized form and CrO$_{x-1}$ represents the reduced form of the catalyst). Based on **Scheme 1**, the by-products of this reaction are CO and H$_2$O, whereby CO can easily react with H$_2$O producing valuable hydrogen via the water gas shift reaction:

- -

$$C_3H_8 + CrO_x \leftrightarrow CrO_{x-1} + C_3H_6 + H_2O \qquad (2.2)$$

$$CO_2 + CrO_{x-1} \leftrightarrow CO + CrO_x \qquad (2.3)$$

$$H_2 + CrO_x \leftrightarrow CrO_{x-1} + H_2O \qquad (2.4)$$

$$CO_2 + CrO_{x-1} \leftrightarrow CO + CrO_x \qquad (2.5)$$

SCHEME 1 | CO$_2$-ODH of propane to propylene over chromium oxide catalytic sites.

- -

The consequence of promoters, such as Fe, Co, and Mn oxides, on Cr-based Cr$_2$O$_3$/ZrO$_2$ nano-composite catalysts for CO$_2$-ODH of ethane was found to distinctly enhance ethylene selectivity (Deng et al., 2007). It was observed that weak acid sites promote the ethylene formation through improved ethane activation, whereas

strong acid–base sites favor the undesired reactions of reforming and ethane cracking (Deng et al., 2007). In addition, the oxygen species types, i.e., the lattice oxygen (O_I), oxygen in adsorbed CO_2 or carbonates (O_{II}), and adsorbed oxygen species (O_{III}), can influence the reaction rate and ethylene selectivity. Lattice oxygen species are responsible for selective oxidation of hydrocarbons, whereas the adsorbed oxygen species result in more CO_x formation due to deep oxidation (Pena and Fierro, 2001; Deng et al., 2007). Catalysts, such as $Na_2WO_4/Mn/SiO_2$, suitable for oxidative coupling of methane reaction are also active in the ODH of ethane (Pak et al., 1998). In fact, Han et al. (2010) patented a mixed valent catalyst system comprising synthetic cryptomelane or octahedral molecular sieve with Fe as the transition metal for the CO_2 dehydrogenation of ethane at 550°C in order to produce ethylene and CO mixtures, which are used as feedstock for the ethylene homologation to propionic acid derivatives.

The catalytic properties of vanadium oxide correlate to the supports' acid–base nature (Blasco et al., 1995) as well as on the vanadium dispersion on the support (Liu et al., 2004). Raju et al. (2012) synthesized V_2O_5 supported on various mixed oxides, such as $SnO_2–ZrO_2$, $CeO_2–ZrO_2$, and $TiO_2–ZrO_2$ (Raju et al., 2014). The high surface area and superior acid–base bifunctionality of $SnO_2–ZrO_2$ supported V-catalyst were found to demonstrate good catalytic activity compared to vanadia supported on single oxides. The nature of the support strongly affects reducibility of V_2O_5. However, in the case of $CeO_2–ZrO_2$ supported V_2O_5, despite the slightly lower conversion caused by $TiO_2–ZrO_2$ and $SnO_2–ZrO_2$ supported catalysts, the total selectivity toward butylene is much higher with the main reason being participation of larger amounts of lattice oxygen species and oxygen vacancies (which are replenished by CO_2) forming $CeVO_4$ species (Raju et al., 2014). Evidently this is due to the redox nature of $CeO_2–ZrO_2$ supports that increases oxygen mobility and facilitates oxidation/reduction of the Ce^{4+}/Ce^{3+} couple (de Lima et al., 2008; Postole et al., 2010).

Mesoporous structured supports, such as MCM-41 or SBA-15, are highly favorable to improve catalyst dispersion. As such impregnation of vanadium on mesoporous siliceous MCM-41 was found to result in greater density of surface-active sites owing to large pore diameters and the stronger interaction, which exists between the active species and its support compared to amorphous silica (Solsona et al., 2001). Furthermore, the thicker walls (31–64 Å) of SBA-15 types of mesoporous silica compared to their MCM-41 counterparts lead to greater thermal and hydrothermal stability (Liu et al., 2004). Isolated tetrahedral vanadium oxide species containing terminal V=O groups well dispersed on the mesoporous silica at predominantly low vanadia content (in order to prevent polymerization) have been identified to be the active sites.

Early studies for ODH of alkanes were focused on co-feeding CO_2 as a promoter along with O_2 in order to improve the dynamic phenomena at the surface of oxides resulting in greater olefin yields. Thus in these works, CO_2 acted as a modulator of the oxidative properties of oxygen (Dury et al., 2003a; Park and Ansari, 2013). Among the advantages of CO_2 introduction in the system are lower tendency for hydrocarbons combustion (whilst minimizing hot spot formation) and decrease in coking effect (Dury et al., 2003b).

Urlan et al. (2008) reported that the ODH of n-butane over titanium pyrophosphate (TiP_2O_7) can be enhanced by co-feeding CO_2 in the system. However, feeding CO_2 only caused lower conversions. Similarly, increasing CO_2 partial pressures over V–Mg–O catalysts improved yield and selectivity of C_4 dehydrogenation products (Ge et al., 2003).

The molybdenum oxide-based catalysts possess a chemistry comparable to that of vanadium oxide, due to the fact that Mo can be present as MoO_x monomers, polymers, or MoO_3 crystallites. The various forms of Mo depend on the loading, support type, and catalyst preparation methods (Sattler et al., 2014). For example, in a Mo_2C/SiO_2 system, by co-feeding CO_2 for the ODH reaction, the benefits of CO_2 in oxidizing the Mo_2C forming Mo-oxycarbide at higher temperatures could be observed (Solymosi and Nemeth, 1999; Solymosi et al., 2001). In fact, Dury et al., 2003a) reported that dissociation of CO_2 on the catalyst surface could take place due to introduction of 3% CO_2 for the ODH reaction of propane over $NiMoO_4$ hence inducing the oxidation of molybdenum suboxide at temperatures around 673–723 K. The presence of both molybdates and molybdenum oxides can enhance the catalytic properties of $NiMoO_4$ in hydrocarbon oxidation (Lezla et al., 1997; Dury et al., 2003a). CO_2 dissociation results in formation of oxygen species that have higher selectivity compared to molecular oxygen and radical formation can be avoided.
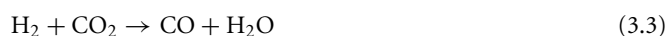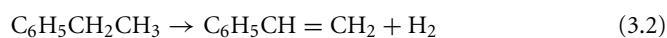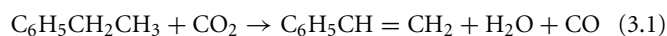
OXIDATIVE DEHYDROGENATION OF ETHYLBENZENE TO STYRENE

The ODH of ethylbenzene (ODE) to styrene reaction is growing rapidly as a promising alternative to the current steam-based process in view of the increasing demand of styrene and its rapid market growth (Castro et al., 2013). Styrene is an important precursor for high-value commercial products such as synthetic rubbers, polystyrene, and styrene–acrylonitrile copolymers (Ba et al., 2014). Industrially, excess of steam is required for ethylbenzene dehydrogenation to styrene to overcome both carbon deposition and reaction thermodynamics (Jiang et al., 2009; Pramod et al., 2014). However, being a highly endothermic process, the conversion rarely exceeds 50%. Furthermore, the production of toluene, benzene, and coke, due to side reactions, also affects the process yield and selectivity, and leads to catalyst deactivation (Rangel et al., 2012). As aforementioned, the deep oxidation and radical formation associated with oxygen as the dehydrogenation agent led to growing use of CO_2 as dehydrogenating agent, in order to enhance styrene selectivity (97%) and prevent hot spots (de Araujo et al., 2010; Irún et al., 2013). Via the use of CO_2, the explosion risks associated with use of oxygen can be mitigated besides ensuring high selectivity toward styrene production (Park et al., 2005).

Park et al. (2005) in their invention described the process of utilizing CO_2 as a soft oxidant for the dehydrogenation of alkylaromatic hydrocarbons, such as ethylbenzene, in the presence of heterogeneous catalysts containing vanadium and iron in various configurations. As compared to the conventional processes, utilization of CO_2 as a "soft oxidant" enables operation at a lower temperature and provides significant energy savings along with improved conversion (Park et al., 2005). In fact, the energy consumption for the CO_2-based ODE process compared to steam-based is about $1.5–1.9 \times 10^5$ instead of 1.5×10^6 kcal/mol of styrene produced

(Rangel et al., 2012). In a more recent invention described by Schwint and Wilcox (2009), the process information is described in detail. In summary, the CO$_2$ required for the dehydrogenation of ethylbenzene to styrene monomer can be supplied externally from the release of another petrochemical process as a recycle stream. The process steps include details on addition of steam, hydrogen, methane, or other hydrocarbon fuel to the recycle carbon dioxide stream. The CO$_2$ and ethylbenzene stream is heated in a heat exchanger and fed to an oxidizer having a selective oxidation catalyst. Two-stage oxidizer and two-stage dehydrogenation reactors coupled with heat exchangers are used for the conversion of ethylbenzene to styrene. With the presence of CO$_2$ in the feed stream, the superheated steam used for the heat exchangers is required in lower quantities than conventional ethylbenzene dehydrogenation processes. A distillation column is used to separate the dehydrogenation product mixture from the styrene monomer (Schwint and Wilcox, 2009).

Based on **Scheme 2**, the overall process is shown in Eq. 3.1, whereas the two-step pathway is presented in Eqs 3.2 and 3.3 as follows (Mimura and Saito, 2000):

- -

$$C_6H_5CH_2CH_3 + CO_2 \rightarrow C_6H_5CH = CH_2 + H_2O + CO \quad (3.1)$$
$$C_6H_5CH_2CH_3 \rightarrow C_6H_5CH = CH_2 + H_2 \quad (3.2)$$
$$H_2 + CO_2 \rightarrow CO + H_2O \quad (3.3)$$

SCHEME 2 | Pathway schematic for CO2-ODE to styrene.

- -

Based on Eq. 3.3, the produced hydrogen from the dehydrogenation step is removed as steam by the reverse water gas shift (RWGS) reaction to further shift reaction equilibrium. The simultaneous removal of coke via CO$_2$ gasification ensures minimization of carbon deposition and generation of undesired CO$_x$ species.

In another recent patent invention, Arnold et al. (2014) described a process of incorporating oxygen (via an oxygen selective membrane reactor, preferably made from fluorite or perovskite-based mixed oxides) along with CO$_2$ to promote ODE to styrene. The oxygen sources can be from high- or low-purity O$_2$, enriched and atmospheric air. In fact, the supplemented oxygen can provide partial exothermic heat to the reaction, thus lowering the energy requirement of this reaction, besides maintaining the high selectivity afforded by CO$_2$ (Arnold et al., 2014). The presence of an oxygen selective membrane reactor can provide advantages, such as continuous injection of oxygen from various points along the membrane reactor, thus minimizing the probability of hot spots in the catalyst bed. This invention was followed by a more comprehensive process configuration, which is inclusive of a separator section including condenser, compressor, and water as shift unit capable of converting the CO contained in the off-gas stream to more H$_2$ and CO$_2$ in order to recycle back the CO$_2$ into the process. Moreover, a multi-function catalyst capable of simultaneous hydrocarbon dehydrogenation as well as CO oxidation (preferably noble metal based) is utilized in this process (Arnold et al., 2014).

CATALYTIC SYSTEMS FOR CO$_2$-ODE TO STYRENE

Redox nature and acid–base properties of the catalyst are several factors, which are important to improve selectivity toward styrene production. Early research showed that iron catalysts on various supports, such as alumina and activated carbon, are promising for enhanced styrene selectivity in the CO$_2$-mediated ODE reaction (Badstube et al., 1998; Mimura and Saito, 2000). However, the existence of some disadvantages, such as low-surface area and susceptibility toward deactivation of the catalytically active Fe^{3+} sites, propelled the need for promoters, such as titania (de Araujo et al., 2010; Castro et al., 2013). For example, among the promoters, such as Ti, Al, and Zr, Ti modification showed much promise (Castro et al., 2013). Formation of FeTiO$_3$, Fe$_2$TiO$_5$, and FeTi$_2$O$_5$ stable mixed oxide phases improved resistant against phase transformation and sintering and, thus, assuring high catalytic performance. However, styrene oligomerization occurred while the formation of carbon was increased due to ethylbenzene cracking (Castro et al., 2013).

Iron oxide doping on ceria-based catalysts can result in formation of Ce$_{1-x}$Fe$_x$O$_2$ solid solutions, which performed better than ceria-based Zr, Ti, Pr, and Y mixed oxides (Wang et al., 2014a). The Ce$_{1-x}$Fe$_x$O$_2$ solid solutions were synthesized *via* the hydrothermal method resulting in a highly dispersed Fe$_2$O$_3$ on the surface of the Ce stabilized structure (Wang et al., 2014a). Raman analysis was used to confirm the solid solution formation with Fe^{3+} in the CeO$_2$ lattice. Even though Fe^{3+} doping can potentially improve the reaction kinetics (Wang et al., 2014a), however, it has a lower energy for the formation of oxygen vacancies, compared to the un-doped system. These oxygen vacancies are crucial in promoting rapid oxygen exchange between Ce^{4+} and Ce^{3+} redox sites (improving oxygen storage capacity of ceria), thus enabling iron to maintain its high shift activity promoting. In addition, CO$_2$ adsorption and activation were enhanced leading to a 13% higher conversion values (Reddy et al., 2012).

Another widely investigated series are the vanadium-based catalysts. By substituting vanadium in Mg–Al hydrotalcite catalysts, the Mg–V–Al mixed oxides with high surface area and mesoporous characteristics were produced, and found to be favorable for the ethylbenzene dehydrogenation to styrene under CO$_2$ flow (Carja et al., 2003). Moreover, V^{5+} was identified to be the active site for the dehydrogenation process (Carja et al., 2003). The major properties of this catalyst are the weak Lewis acid sites contributed by aluminum, which reduce the catalyst deactivation, in addition to its high surface area contributed by the mesoporous characteristics.

Vanadium was also doped on titanium oxide using the acid-catalyzed sol gel technique, which was shown to be an effective technique to systematically synthesize the catalyst at the required ratio (Li et al., 2009). The authors demonstrated that the optimal loading of 6 mol% V^{5+} resulted in diminution of the particle size favoring formation of small crystallites, caused by incorporation of vanadia into TiO$_2$.

Capitalizing on the oxygen vacancy effect, Rao et al. (2009) and Burri et al. (2013) investigated the effect of ceria on the structure and catalytic CO$_2$-ODE reaction activity of V$_2$O$_5$/TiO$_2$–ZrO$_2$ catalyst. This research group had previously noted that titania–zirconia mixed oxides exhibited excellent catalytic activity

and selectivity for the CO$_2$-ODE to styrene reaction in view of the high specific surface area, good acid–base and redox properties, coupled with the mechanical and thermal stabilities of the TiO$_2$–ZrO$_2$ mixed oxides (Burri et al., 2007; Reddy et al., 2008). In their catalyst system, the formation of crystalline ZrTiO$_4$ spinel phase along with ZrV$_2$O$_7$ and CeVO$_4$ phases was also observed. A high product selectivity of 98% and ethylbenzene conversion of 56% were obtained over the ceria-doped catalyst. The presence of ceria was found to be critical in retarding the catalyst deactivation rate due to its redox properties, which minimized carbon deposition.

In addition, Burri et al. (2007) have also explored the use of high surface area mesoporous silica, such as SBA-15 supports for the redox-based CeO$_2$–ZrO$_2$ mixed oxide catalysts. A significant enhancement in ethylbenzene conversion from 21 to 65% at reaction temperatures ranging from 723 to 923K could be observed in their catalyst system. The catalyst redox nature ensured greater oxidation–reduction activity at the higher temperatures based on the surface changes, which evolved and resulted in greater availability of surface oxygen (Burri et al., 2007).

MCM-41, another type of mesoporous silica, has also been employed as a high surface area support for vanadia catalysts (Qiao et al., 2009). An improved catalyst dispersion on the mesoporous silica compared to the conventional silica support was proven by Raman spectra, which showed the presence of strong bands of isolated tetrahedral VO$_4$ (Qiao et al., 2009).

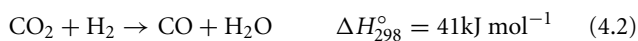## CO$_2$ (dry) REFORMING OF HYDROCARBON/ALCOHOL
CO$_2$ REFORMING OF METHANE
Methane is the simplest hydrocarbon molecule, of which hydrogen is the main product. Steam reforming of methane is the most common reaction, which is in industrial application. However, in view of global warming phenomenon due to excessive greenhouse gas emission, CO$_2$ dry reforming of methane (DRM) has emerged as an attractive alternative. DRM reaction results in production of syngas (consisting of H$_2$ and CO in the ratio of 1:1) (Eq. 4.1) and can be used as an important feedstock for industrial processes, such as hydrocarbonylation and hydroformulation reactions (Vasant and Kartick, 2006).

Dry reforming of methane is a highly endothermic reaction (Eq. 4.1), and thus performs better at higher temperature especially in the range between 700 and 900°C (Bradford and Vannice, 1999):

$$CO_2 + CH_4 \rightarrow 2CO + 2H_2 \qquad \Delta H^{\circ}_{298} = 247 \, kJ \, mol^{-1} \quad (4.1)$$
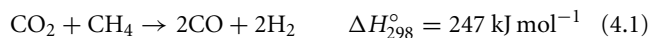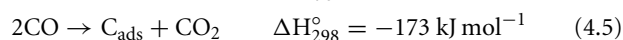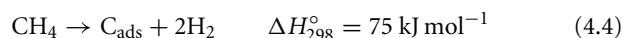
The main side reaction involved is the simultaneous occurrence of RWGS reactions (Eq. 4.2) that produces more CO. The steam produced plays a role in gasifying carbon deposited in the reaction (Eq. 4.3):

$$CO_2 + H_2 \rightarrow CO + H_2O \qquad \Delta H^{\circ}_{298} = 41 kJ \, mol^{-1} \quad (4.2)$$

$$C + H_2O(g) \rightarrow CO + H_2 \qquad \Delta H^{\circ}_{298} = 31 \, kJ \, mol^{-1} \quad (4.3)$$

Methane dissociation (Eq. 4.4) as well as CO disproportionation (Eq. 4.5) is the main reactions involved in carbon deposition,

which causes eventual catalyst deactivation and plugging of the reactor (Zhu et al., 2008):

$$CH_4 \rightarrow C_{ads} + 2H_2 \qquad \Delta H^{\circ}_{298} = 75 \, kJ \, mol^{-1} \quad (4.4)$$

$$2CO \rightarrow C_{ads} + CO_2 \qquad \Delta H^{\circ}_{298} = -173 \, kJ \, mol^{-1} \quad (4.5)$$

Transition metal catalysts, such as Ni, are known to be highly active in the catalytic DRM reaction and comparable to noble metal catalysts. However, the transition metal catalysts are susceptible to carbon deposition (Wang et al., 2014b). Therefore, great importance is placed on design and synthesis of highly active, stable, and economically viable catalyst system, which can inhibit the coke formation while maintaining high catalytic activity for the DRM reaction.

Van et al. (2006) described a process for the combined reforming of steam with CO$_2$ for hydrocarbon reforming. The process temperature is maintained by routing part of the hot product gas from partial oxidation reaction which takes place at the exterior of the reactor tubes in the reactor vessel. In general most of the processes for steam reformers can be adapted for CO$_2$ reforming. In terms of reactor design, the inner passageways are metal conduits aligned co-axially with the reactor conduit, and are capable of facilitating heat transfer (from partial oxidation reaction) to the reformer. In a recent invention, Olah and Prakash (2013) advocated the method of forming methanol, in which the DRM reaction is combined with the conventional steam reforming of methane at a specified ratio in a process described as bi-reforming reaction. In this reaction, the methane, CO$_2$, and water are reacted in the ratio of 3:2:1 as shown below:

$$3CH_4 + 2H_2O + CO_2 \rightarrow 4CO + 8H_2$$

The bi-reforming reaction catalyzed on a Ni-supported on high surface area or nanostructured support is able to suppress coke formation and produces syngas in the ratio of 2H$_2$:CO (Olah and Prakash, 2013). This ratio is the right amount required for methanol production, which is used as a building block in the chemical industry. Besides, methanol also provides an environmentally friendly alternative to diesel fuel due to its cleaner emission.

In order to ensure thermoneutrality of the process, air/O$_2$-rich gas can be supplied to the system. In fact, Saudi Arabian Oil Co. has filed for a patent application on the utilization of a multicomponent catalyst system comprising Ni, Rh, Re, and Pt metals with Ce$_2$O$_3$, La$_2$O$_3$, and ZrO$_2$ mixed oxides to reform petroleum fuel to H$_2$-rich syngas. Combustion, steam, and/or CO$_2$ reforming of the petroleum-based fuel is carried out simultaneously in the interior zone of a reactor for syngas production (Al-Muhaish et al., 2015).

Noble metals
Dry reforming of methane process generally is catalyzed by either noble metals (Rh, Ir, Pt, Rh) or some transition metal catalysts, such as Ru and Ni. Noble metals are used for their resistance to corrosion and oxidation, high activity, and good carbon resistance (Obradovic et al., 2013).

A series of noble metal catalysts (Rh, Ru, Ir, Pt, and Pd) supported on alumina–magnesia spinel compound was studied by Rezaei et al. (2006). Rhodium and ruthenium were shown to exhibit high activity and stability compared to the rest. This was attributed to the formation of more reactive carbon, which was identified as C_γ or superficial carbide. On the other hand, the lower stability of Pd catalyst was caused by the formation of less reactive whisker carbon. Zhang et al. (1996) studied the effect of Rh catalysts and found the specific activities to be strongly dependent on catalyst support as well as the metal particle size (Zhang et al., 1996). In general, the activities were found to increasing with metal particle size. By using different kinds of support, it was found that the deactivation rates showed decreasing order of $Rh/TiO_2 >> Rh/Al_2O_3 > Rh/SiO_2$. The poor stability of Rh/TiO_2 was attributed to its strong metal support interaction (SMSI) effect, whereas the inert nature of the SiO_2 support resulted in an almost negligible metal support interaction.

Yokota et al. (2002) were another group who studied the effect of Rh catalyst and found that higher surface area supports were vital to improve Rh dispersion. With increasing Rh dispersion, turn over frequency (TOF) was found to decrease. Therefore, TOF for CH_4 conversion decreased in the order of $Rh/TiO_2 > Rh/La_2O_3 = Rh/CeO_2 > Rh/ZrO_2 = Rh/MgO = Rh/SiO_2 = Rh/MCM-41 > Rh/\gamma-Al_2O_3$. Detailed investigations using XANES revealed that Rh existed as metal on TiO_2 whereas Rh on Al_2O_3 possessed a cationic character. This led to a conclusion that Rh was structure sensitive in DRM reaction.

Mark and Maier (1996) found that TOF over Rh, Ru, Ir, Pt, or Pd-supported catalysts did not significantly depend on metal dispersion, which is in contrast with the results of Yokota et al. (2002). They observed that the support was only influencing the stabilization of metal surface area, which was responsible for the catalyst activity. Hence, they postulated that under reaction controlled temperatures, it was sufficient to consider only the accessible metal surface area.

Erdöhelyi et al. (1994) conducted an in-depth investigation on Pd-based catalyst for CO_2 reforming of methane. According to them, the decomposition of methane resulted in yielding hydrogen and small amounts of ethane and ethlyene. Although carbon deposition was observed, however, at the stoichiometric feed ratio (1/1) of CH_4 and CO_2, the amount was rather low. Therefore, they concluded that at high reaction temperatures, Pd supported catalysts exhibit high catalytic activity with no or only very little carbon deposition.

Platinum (Pt) supported catalyst was also widely investigated for the DRM reaction. Souza et al. (2001, 2002) investigated on Pt/Al_2O_3 and Pt/ZrO_2 catalysts for DRM reaction. They found that Pt/Al_2O_3 catalyst showed fast deactivation during DRM reaction as a result of high carbon deposition rate. However, by introducing a small amount of ZrO_2 (>5%) to Pt/Al_2O_3 catalyst, the activity and stability were tremendously improved. The presence of $Pt–Zr^{n+}$ interfacial sites was the main reason attributed to low carbon deposition, which rendered higher stability and activity of ZrO_2 promoted Pt/Al_2O_3 catalyst. In fact, Bitter et al. (1999) and Nagaoka et al. (2001) also reported that the stability of Pt catalysts increased in the order of $Pt/ZrO_2 > Pt/TiO_2 > Pt/\gamma-Al_2O_3$, whereas the carbon formation rate decreased in the order of $Pt/ZrO_2 < Pt/TiO_2 << Pt/\gamma-Al_2O_3$. Hence, even though Pt is a noble metal, these findings indicate that deposition of carbon which blocks the active metal site was the main cause of deactivation of the platinum-supported catalysts.

In addition, there have been studies on the low metal loadings of the noble metals as means of reducing the implications of cost. For instance, Bitter et al. (1999) utilized a loading as low as *ca.* 0.5–1 wt% Pt on zirconia to study deactivation and coke accumulation during DRM reaction. They found that the size of the Pt particles and the stability of the carbonates formed on the support (from CO_2 activation) to be the critical factors in influencing carbon formation rate. Smaller Pt particles as well as supports favoring carbonate formation are favorable in promoting the catalyst stability during the DRM reaction.

Ni supported metal oxide
However, in order to enhance the catalytic performance, without doubt higher loadings of active metals are required. Nickel, among non-noble metals, is the only one from Group 8 transition metals that has comparable activity to noble metals (Gao et al., 2011). Nevertheless, as aforementioned, nickel catalysts are more susceptible to catalyst deactivation due to carbon formation. As such, an immense requirement for investigation on suitable catalyst supports or promoters to be used to eliminate the extensive carbon formation on Ni-based catalysts.

Several studies have been carried out in order to rationally synthesize Ni-based catalysts in order to provide high activity and improved carbon resistance. Some of the nickel-based catalysts synthesized include bimetallic catalyst, supported Ni catalyst, perovskite-based and Ni core–shell structured catalysts.

According to Ruckenstein and Hu (1996), addition of various promoters, such as La_2O_3, MgO, BaO, and CaO to the catalyst system are found to benefit DRM activity in terms of decreasing coke formation (Pakhare et al., 2014). Similarly, Zhao and Wagner (2004) have patented the calcium promoted Ni supported on calcium aluminate catalyst for the CO_2-steam reforming of methane. The Ni supported on calcium aluminate catalyst was found to be not only coke resistant, but also able to tolerate sulfur compounds at concentrations between 1 and 20 ppm. The calcium promoter was able to enhance the catalyst surface and porosity and displayed higher activity index compared to conventional Ni supported on alumina catalysts. Moreover, addition of these promoters can result in strong metal–support interaction, as well as lattice oxygen mobility, which are of prime importance in this reaction. For example, promotion of Ga_2O_3 on inert SiO_2 support resulted in activation of CO_2, thus forming surface carbonate and hydrogen carbonate species which provided higher catalytic stability and coke resistance on Ga_2O_3-promoted SiO_2-supported Ni catalyst (Pan et al., 2010). In another study, Mo et al. (2014) studied the effect of La_2O_3 on SiO_2 supported Ni nano-catalyst. The Ni nano-catalyst was synthesized using a facile and economical *in situ* self-assembled core–shell precursor route via incipient wetness co-impregnation method. In this method, oleic acid was used to ensure formation of Ni nanocatalysts with particle sizes less than 3 nm. The catalytic DRM performance could be significantly improved with promotion of only 1 wt% La_2O_3, whereby near equilibrium CO_2 and CH_4 conversions (above 80%) at 973 K

could be achieved. Furthermore, due to the good catalyst dispersion, negligible carbon deposition could be attained even after 100 h on stream at gas hourly space velocity of 72,000 g. Similarly, the positive influence of the basic borated–alumina (B_2O_3–Al_2O_3) supported Ni-catalyst profoundly influenced the catalytic DRM performance (Ni et al., 2012). The authors proposed that the surface hydroxyl (OH) groups present on the catalyst surface were crucial in oxidizing surface carbon species from dissociation of methane molecules in order to maintain catalytic stability.

The importance of basicity was explored by another recent investigation on the effect of Sr over the catalytic DRM performance of Ni–La₂O₃ catalysts (Sutthiumporn and Kawi, 2011). The Sr-doped Ni–La₂O₃ catalyst significantly enhanced the DRM process even temperatures as low as 873 K coupled with low carbon deposition. The highly mobile surface oxygen species present on the catalyst system played an important role in C–H activation for the higher activity, and adsorbing adsorb CO_2 molecules in order to form bidentate carbonate species for carbon removal (Sutthiumporn and Kawi, 2011). Similarly, alkaline promoter, such as magnesium oxide, was also studied on the Ni/La₂O₃ systems. In fact, it is widely known that MgO possess basicity and has the same crystal structure as NiO, hence can easily form the non-reducible basic solid solution of $Ni_xMg_{(1-x)}O$, which is important to improve basicity and catalyst dispersion (Arena et al., 1991). Based on the study by Ni et al. (2013), the loading of 5 wt% Ni on a MgO promoted La₂O₃ support at the optimal mole ratio of 10 Mg^{2+}/La^{3+} resulted in generation of highest amount of monoclinic lanthanum oxycarbonate species and surface adsorbed oxygen ions which are able to oxidize deposited carbon (Ni et al., 2013).

Bimetallic catalysts

Bimetallic structures involves alloying with a second metal (either a noble metal or another transition metal) in order to modulate the catalyst properties by causing a "synergistic" effect between the two metals (Sankar et al., 2012). For instance, the effect of Pd on Ni-based catalysts supported on yttria was tested by Oemar et al. (2011) for the oxidative DRM reaction. The bimetallic Pd–Ni species enhanced the metal support interaction. Furthermore, the presence of α-oxygen on Y_2O_3 surface played an important role in C–H bond scission of CH_4 as well as oxidation of the deposited carbon. However, the surface α-oxygen amount is very low; hence a small amount of oxygen was co-fed for the DRM reaction in order to ensure regeneration of the α-oxygen and thus maintaining the stability of the catalyst.
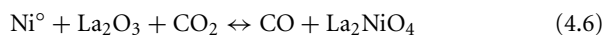
Besides noble metals, other transition metals can also be used to form alloyed bimetallic structures. For example, Zhang et al. (2007b, 2008) synthesized various Ni–Me (Me = Co, Fe, Cu, or Mn) bimetallic catalysts in the hydrotalcite structure of Ni–Co–Al–Mg–O using the coprecipitation method. Ni–Co was shown to exhibit the best results with respect to DRM catalytic stability and activity. A 2000-h DRM catalytic stability test was successfully conducted with negligible catalyst deactivation. This bimetallic catalyst composition containing the dual-active catalyst components of Ni and Co and tested active for DRM was patented by the authors and tested for high gas hourly space velocity between 2000 and 2,000,000 ml/gcat h⁻¹ (Wang et al., 2011). This catalyst system

can be prepared by various techniques including co-precipitation, sol gel, impregnation, and homogeneous precipitation.

Perovskite catalysts

Another group of structured type catalysts, i.e., perovskite-type represented by the general formula ABO_3 have been widely investigated for high-temperature reactions, such as DRM due to their high thermal stability (Pena and Fierro, 2001, Moradi et al., 2014). In general, the B-site cation is surrounded octahedrally and the A-site cation is located in the cavity made between these octahedral sites. The lattice parameter and unit cell dimensions can be modified by A-site ion substitution in these structures offering the possibility of varying the dimensions of the unit cell. Thus, accordingly, the covalence of the B–O bond in the ABO_3 structure can be modified (Fan et al., 2009). Replacement of A- and/or B-site cations by other metal cations leads to formation of lattice defects, which are crucial for O_2-adsorption and oxygen mobility within the crystal structure, in order to promote catalytic activity.

For the DRM reaction, the perovskite catalyst structure generally consists of rare earth elements, such as lanthanum in the A-site, and transition metal elements, such as nickel (active centers for methane activation) in the B-site. According to Batiot-Dupeyrat et al. (2003), the $LaNiO_3$ perovskite-type oxide is reduced under hydrogen atmosphere in three steps. In the first reduction step (200–500°C), $La_4Ni_3O_{10}$ phase is formed, while the second step (600–650°C) leads to the formation of the spinel-type La_2NiO_4 phase. The final step (680–750°C) coincides with decomposition into La_2O_3 and Ni metal. The consecutive reaction steps are summarized as shown below:

$$Ni° + La_2O_3 + CO_2 \leftrightarrow CO + La_2NiO_4 \qquad (4.6)$$

$$CH_4 + La_2NiO_4 \rightarrow CO + 2H_2 + La_2O_3 + Ni° \qquad (4.7)$$

The well-defined perovskite structure and their interesting redox properties and accessibility enable attainment of nanometer sized metallic particles under reducing environment (Valderrama et al., 2010). Thus, this leads to desirable properties to maintain catalytic activity and stability under the high-temperature reaction environment. The La_2NiO_4 perovskite-type catalyst (with A_2BO_4 structure) was found to demonstrate higher catalytic activity compared to supported Ni/La₂O₃ or LaNiO₃ catalyst due to formation of even smaller nickel particle after reduction (Gallego et al., 2006). The reduction treatment is an important parameter to mitigate carbon deposition on the La_2NiO_4 catalyst. This is due to limitation in La_2O_3 sites for the un-reduced La_2NiO_4 catalyst, which resulted in lower CO_2 activation in order to completely facilitate carbon removal.

In fact, both the A-site and B-site of the perovskite catalyst can be substituted in order to enhance the catalyst performance. Sutthiumporn et al. (2012) found that lattice oxygen species in the partially substituted $La_xSr_{1-x}Ni_yMe_{1-y}O_3$ (Me = Fe, Cu, Co, Bi) perovskite catalysts are crucial in activating the C–H bond of the CH_4 molecule for improved reactant conversion at lower temperature DRM reaction. In addition, carbon formation can be suppressed due to the reaction with CO_2 to form $La_2O_2CO_3$. Substitution of Cu to the $LaSrNiO_3$ catalyst was found to initially display high CH_4 conversion; however, particle agglomeration

resulted in subsequent carbon formation causing lower catalytic stability. On the contrary, substitution of Fe resulted in high activity and stability at prolonged reaction time (despite low initial activity) owing to increased mobility of lattice oxygen species under the reducing reaction environment.

Spinel-type oxide Ni-based catalysts of formula ABO$_4$ or A$_2$BO$_4$ are variations to the structured cubic perovskite (Corthals et al., 2008). The sub-stoichiometric spinel structures possess high activity due to high dispersion of NiO into the spinel and thermal stability. Gallego et al. (2008) exhibited high catalytic activity using reduced La$_2$NiO$_4$ as catalyst precursor for DRM at 973 K, with a conversion rate of 85 and 93% for CH$_4$ and CO$_2$, respectively, and inhibition of carbon formation even after 160 h of experiment. Based on their explanation, the absence of carbon deposition was due to the enhanced reaction between La$_2$O$_2$CO$_3$ and the Ni–CH$_x$ species, thus producing the product syngas. Moreover, formation of the small nickel particles (average diameter of 7 nm) upon reduction was crucial in preventing agglomeration and site for carbon growth.

Spinel structures such as NiAl$_2$O$_4$ formed as a result of high-temperature calcinations result in SMSI (Jimenez-Gonzalez et al., 2015). However, they require high reduction temperature for catalyst activation. Moreover, according to Bhattacharyya and Chang (1994), the γ-alumina in the NiAl$_2$O$_4$ spinel structure formed via solid-state reaction can lead to gradual transformation to the α-phase especially over prolonged reaction time at high-temperatures. This causes a decline in catalyst performance due to sintering of the alumina support. In order to overcome this phenomenon, LaAlO$_3$ perovskite oxide phase was pre-formed on alumina-based support and upon calcinations and further impregnation with Ni, a predominantly "inverse" surface nickel aluminate was formed. The formation of this phase could favorably hinder the phase transformation of the γ-alumina to undesirable lower surface area α-alumina phase (Kathiraser et al., 2013a,b).

Pakhare et al. (2013a) have recently reported the synthesis of structurally stable lanthanum-zirconate pyrochlores (La$_2$Zr$_2$O$_7$). In general, the pyrochlore structures (A$_2$B$_2$O$_7$) are crystalline thermally stable ternary metal oxides with a cubic unit cell. Typically, the A-site is a rare-earth element (such as lanthanum) and the B-site consists of a transition metal element with smaller ionic radius. CO$_2$ activation on La site of the Rh modified lanthanum-zirconate pyrochlore was proven (by means of isotopic pulsing) to take place via formation of three polymorphs (types I, Ia, and II) of La$_2$O$_2$CO$_3$, of which only type II is reactive. The authors have also studied the interesting effects on DRM reaction by promotion with metals, such as Rh, Pt, and Ru in the pyrochlore structure (Gaur et al., 2012; Pakhare et al., 2013b). These effects include (i) formation of vacancies at the O sites during synthesis, which enhance oxygen ion migration, thus minimizing oxidation of deposited carbon and (ii) the ability to isomorphically substitute the catalytically active Rh, Pt, and Ru metals into B-site, whereby they do not sinter at high DRM temperatures (Pakhare et al., 2014).

Core–shell catalysts
Core–shell type of catalysts in the form of metal-at-metal oxide nanoreactor structure has been widely studied for high-temperature reactions due to enhanced resistance to sintering caused by partial blocking by the peripheral silica shells. However, just recently, attempts have been made for investigating such catalysts for DRM reaction. Li et al. (2014a) developed Ni-at-SiO$_2$ core–shell catalysts and investigated effect of shell thickness modifications for the DRM reaction. Formation of nickel phyllosilicate species was found to impart high catalytic stability at 1073 K due to strong interaction between Ni core and silica shell (Li et al., 2014a). In a further progress, Li et al., 2014b) successfully tuned the specific surface area in order to achieve specific surface area controllable Ni-at-Ni embedded SiO$_2$, yolk shell nanocomposites, which lead to higher specific surface area, higher Ni dispersion, and stronger interaction between Ni species and SiO$_2$. The preparation method involved a facile self-templating method via the transformation of Ni phyllosilicate, which displays greater DRM reactivity due to easier access of reactants to Ni active sites. These desirable properties led to improved conversion and high stability even at the lower reaction temperature of 973 K (Li et al., 2014b). Since basicity is an important factor especially for CO$_2$ activation and further carbon gasification, Li et al. (2014c) further treated Ni@SiO$_2$ nanoparticles with Mg(NO$_3$)$_2$ forming Ni–Mg phyllosilicate shell. The treatment duration of 10 h was found to be the optimal treatment time in order to ensure sufficient exposure of active Ni metal, while at the same time, stabilizing the Ni particles. This method was successfully applied for DRM reaction at 973 K, achieving high catalytic activity and stability, with negligible carbon deposition even after 95 h time on stream.

CO$_2$ (dry) REFORMING OF ETHANOL
Besides methane, CO$_2$ reforming of alcohols, especially ethanol have begun to attract considerable research interest in recent years. Ethanol has been proposed as raw material for various applications in recent years, since it can be feasibly produced from various biomass sources, such as energy crops, residual materials from agro-industry or forestry, and organic/gasifiable fractions of municipal solid waste via biochemical processes (Jankhah et al., 2008). Most of the catalytic studies in recent years focus on steam reforming of ethanol. However, the growing interest in CO$_2$ reforming of ethanol augurs well in terms of socio-environmental considerations to reduce greenhouse gases and make this a truly sustainable process.

There are several advantages associated with CO$_2$ reforming of ethanol, such as being renewable, biodegradable and easily transportable, and compared to methane (which is non-renewable and highly explosive), ethanol is comparatively less dangerous and toxic (Wu and Kawi, 2009). Hence, ethanol can be considered as an economically viable alternative green power source, which results in low pollutant emissions and controlled combustion (Tsiakarasa and Demin, 2001). In addition, relatively lower temperatures are required for a thermodynamically favorable reaction, where DRE is thermodynamically favorable above 318°C, compared to DRM (above 642°C) (Puolakka and Krause, 2007).
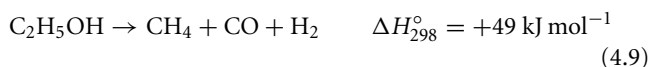
The main reactions involved in DRE are as follows:

$$C_2H_5OH + CO_2 \rightarrow 3CO + 3H_2 \quad \Delta H_{298}^\circ = +339.60 \text{ kJ mol}^{-1}$$
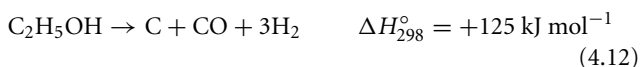
$$(4.8)$$
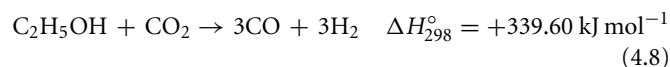
In this stoichiometric reaction, syngas is produced in a theoretical ratio of 1:1, which is similar to DRM process, thus making it suitable for production of some liquid hydrocarbons or oxygenated hydrocarbons (Zhu et al., 2008).

However, other types of side reactions are also prone to take place in parallel during the DRE reaction, such as ethanol decomposition, dehydration reaction, and RWGS reaction (Wu and Kawi, 2009):

$$C_2H_5OH \rightarrow CH_4 + CO + H_2 \qquad \Delta H_{298}^\circ = +49 \text{ kJ mol}^{-1} \tag{4.9}$$

$$C_2H_5OH \rightarrow C_2H_4 + H_2O \qquad \Delta H_{298}^\circ = +45 \text{ kJ mol}^{-1} \tag{4.10}$$

$$CO_2 + H_2 \rightarrow CO + H_2O \qquad \Delta H_{298}^\circ = -39.5 \text{ kJ mol}^{-1} \tag{4.11}$$

Generally, the goal of this reaction is to maximize hydrogen production. Based on the reaction enthalpies, we can see that reaction 4.8 is the most kinetically favored at high-temperatures compared to reactions 4.9 and 4.10 (favored at intermediate reaction temperatures) and reaction 4.11 (favored at low-reaction temperature).

Carbon deposition is also prevalent issue in the DRE reaction and the reactions pertaining to carbon deposition are ethanol decomposition (Eq. 4.12), methane decomposition (Eq. 4.13), ethylene polymerization (Eq. 4.14), and Boudouard reaction (Eq. 4.15):

$$C_2H_5OH \rightarrow C + CO + 3H_2 \qquad \Delta H_{298}^\circ = +125 \text{ kJ mol}^{-1} \tag{4.12}$$

$$CH_4 \rightarrow 2H_2 + C \qquad \Delta H_{298}^\circ = +75 \text{ kJ mol}^{-1} \tag{4.13}$$

$$C_2H_4 \rightarrow \text{Polymerization} \rightarrow \text{Coke} \tag{4.14}$$

$$2CO \rightarrow CO_2 + C \qquad \Delta H_{298}^\circ = -171 \text{ kJ mol}^{-1} \tag{4.15}$$

As we can see, the above carbon producing reactions are mainly from by-products of the initial reactions. In fact, the carbon can be harnessed as carbon nanotube, a material which is rapidly gaining widespread attention due to its many features, such as high porosity, high mechanical strength, high thermal conductivity, low-specific weight, and chemical inertness, and is promising for potential applications in chemistry and physics (Blanchard et al., 2008; Khavarian et al., 2014). Blanchard et al. (2008) described a process whereby CO_2 was reformed with ethanol to syngas and a part of the CO_2 was "sequestered" under the form of carbon nanofibers (CNF) and multi-walled nanotubes (MWNT). Their reaction mechanism was targeted to be as follows:

$$3C_2H_5OH + CO_2 \leftrightarrow 5CO + 9H_2 + 2C \tag{4.16}$$

The formation of carbon during catalytic reforming can be of various types, i.e., graphitic, amorphous, resinous, coal-like, filamental, and nanotubes. Hence, it is crucial that in order to obtain optimally pure and homogeneous of the end product, preconditioning, and optimal setting of reforming parameters, such as reaction temperature, gas hourly space velocity, and catalyst particle size is crucial in affecting the condition of the deposited carbon (Rostrup-Nielsen et al., 2002; de Llobet et al., 2015). In fact, based on a cost analysis conducted by Abatzoglou et al. (2006), it was estimated that the break even cost for a techno-economically sustainable process of multi-walled carbon nanotube production from ethanol dry reforming can reach a price of around US$1.0/kg carbon nanotube. From the reaction (4.16) quoted, carbon formation is targeted along with syngas.

In these reforming conditions, the syngas ratio is lower than the complete dry reforming process (Eq. 4.1), but it sequesters the CO_2 carbon in an inert solid form, which is readily removable from the non-porous catalyst surface (Abatzoglou et al., 2006). Therefore, if the quality of the carbon sequestered is high enough in the form of carbon nanotubes, then it would constitute a major revenue source besides synthesis gas as energy vector or raw material for chemicals synthesis and also the associated carbon sequestration credits (Abatzoglou et al., 2006).

However, when syngas production is the desired outcome, it should be noted that higher hydrocarbons generate more carbonaceous species. For example, via steam reforming reactions, thermodynamic calculations reveal that 1.17 mol C/mol butanol could be observed at 573 K (for steam reforming of butanol at water-to-butanol ratio of 1) compared to 0.58 mol C/mol ethanol at the same conditions for steam reforming of ethanol (Wang, 2011). Operational parameters can further influence the outcome of the reaction. For example, the effect of temperature on carbon formation was analyzed thermodynamically by Jankhah et al. (2008), and thermodynamically, a drastic drop in carbon yield takes place above 550°C, especially at greater CO_2/ethanol ratio at temperatures above 750°C.

Catalyst selection for DRE

Similar to DRM reaction, noble metals and Ni-based catalysts play an important role in the catalytic conversion of DRE reaction, whereby optimization studies of these catalysts are important in order to achieve high activity and selectivity, as well as overcome catalyst deactivation.

In terms of noble metal catalysts, Rh has been shown to display high activity, stability, and low coke formation for the CO_2 reforming of methane and steam reforming of ethanol reactions. In fact, in terms of steam reforming of ethanol, the order of activity for metals is as follows: Rh > Pd > Ni ~ Pt (Wu and Kawi, 2009) As such, Wu and Kawi (2009) studied the DRE reaction with ultra-low loading of 1 wt% Rh supported on Ce incorporated SBA 15 catalysts. As aforementioned, the main benefits of mesoporous silica supports such as SBA 15 are their high surface area, uniform pore size which is tunable from 4.6 to 30 nm and thick wall (around 4 nm) (Wu and Kawi, 2009); which place emphasize on their enhanced stability rendering properties. Furthermore, by incorporating Ce in the SBA 15 structure, the surface oxygen mobility of the catalyst surface can be enhanced due to the redox ability of the $Ce^{4+} \leftrightarrow Ce^{3+}$ species (Lee et al., 2008). The key factors behind the successful implementation of Rh/Ce-SBA 15 catalysts for syngas production from dry reforming of ethanol (DRE) are due to the mobility of surface oxygen species (attributed to Ce incorporation in SBA 15) as well as the good dispersion of Rh over

the Ce/SBA 15 catalyst support. The highest amount of hydrogen production was achieved at the optimal Ce/Si molar ratio of 1/20. Even upon increasing the reaction temperature up to 750°C, the hexagonal mesopores of the Ce/SBA 15 structure was found to remain intact.

In another study, CO$_2$ as a co-feed to ethanol steam reforming was carried out over Pt/ceria catalysts (de Lima et al., 2010). Compared to Ni-based catalysts, carbon diffusion does not take place on noble metals, however, carbon may encapsulate the metal particle or cover the support, thus causing catalyst deactivation. In view of this, de Lima et al. (2010) studied the effect of adding CO$_2$ to the feed in order to shift the equilibrium in favor of the reactants, which can help mitigate carbon deposition. Via this approach, they proposed that CO$_2$ may be recirculated from the outlet stream of the proton exchange membrane fuel cell. The positive effects of CO$_2$ in favoring catalytic stability and favoring formation of CO and acetaldehyde over carbon deposits were clearly demonstrated based on the IR bands obtained over DRIFTS spectra. In brief, the ethoxy species undergo ODH to acetate via addition of O provided by the support from species such as by bridging OH group (during steam reforming) or O adatom by CO$_2$ dissociation at vacancies (during dry reforming). Hence, the acetate further undergo demethanation to form carbon intermediates and further reform CH$_x$ species. Hence, a carbon cleaning mechanism is proposed by the authors, whereby CO$_2$ competes with ethanol for the same adsorption sites, thus reducing the rate of decomposition of the adsorbed intermediate species. Hence, this was found to directly impact rate of CH$_x$ species formation, thus reducing catalyst deactivation, by enhancing more CO production (de Lima et al., 2010).

Hu and Lu (2009) have studied the DRE reaction over conventional Ni/Al$_2$O$_3$ catalysts. Based on their observations, at CO$_2$/ethanol ratio of 1, ethanol decomposition dominates, leading to CO/H$_2$ ratio much lower than 1. In order to enhance reforming of ethanol, increasing CO$_2$/H$_2$ ratio to 5, resulted in lowered production of side products such as CH$_4$, acetaldehyde and coke, and facilitated DRM and coke gasification. They postulated that employing excess CO$_2$ at high-temperatures could enhance the efficiency of coke elimination and resulted in selectivity toward more syngas production. These observations were consistent with Bellido et al. (2009) who investigated the performance of Ni/Y$_2$O$_3$–ZrO$_2$ supported catalysts for DRE at various temperatures and reported that greater selectivity toward syngas production could be achieved by manipulations of the system parameters and reaction conditions. This was because carbon accumulation blocks the metallic active sites and enhances ethanol dehydration and thermal decomposition of ethanol, which increases the methane and C$_2$H$_4$ production.

Recently, Zawadzki et al. (2014) studied DRE reaction over Ni supported on Al$_2$O$_3$, CeO$_2$, MgO, and ZrO$_2$ by impregnating the oxide with a solution of Ni(NO$_3$)$_2$ in methanol. Their study was aimed to verify the use of methanol in the preparation method and its effect on the different oxide-based supports. Ni/Ce was found to result in higher syngas production compared to Ni/Al, Ni Zr, and NiMg catalysts. However, NiCe also showed the highest proportion of filamentous carbon species compared to amorphous

carbon compared to the rest of the catalysts, proven based on Raman and SEM analysis. The fine dispersion of Ni^o on this sample characterized by the smaller Ni^o particles suggest the favoring toward formation of filamentous carbon at low growth rate, due to the low driving force for carbon diffusion through small crystals (Zawadzki et al., 2014).

Carbon steel catalysts have also been explored for the DRE reaction for hydrogen and carbon nanotube production. Oliveira-Vigier et al. (2005) investigated the use of recyclable and long-lasting SS 316 catalyst for DRE reaction and successfully obtained a hydrogen yield that is 98% of the theoretical value. Likewise, Blanchard et al. (2008) and Jankhah et al. (2008) have also used carbon steel catalyst to evaluate the production of syngas and nanocarbons via DRE. High yields of hydrogen and carbon could be produced at the relatively low temperature of 550°C. In summary, ethanol decomposition and dry reforming were the main reaction pathways for the production of hydrogen and carbon nanotube via carbon steel catalyst for the DRE reaction. Based on the TEM results of carbon nanofilaments (CNFs) obtained from ethanol dry reforming, Jankhah et al. (2008) concluded the following:

(1) The CNFs consist of graphite sheets that not concentric to the internal empty tube, but instead are rather oblique to the tube axis.
(2) The CNFs are both in the form of rectilinear and helicoidally arranged, and in certain cases, each CNF contain more than one grain.
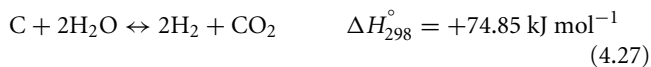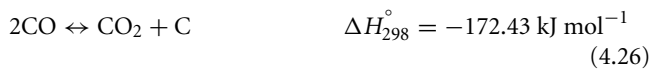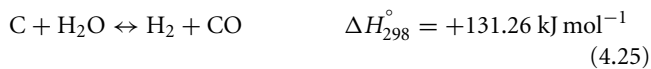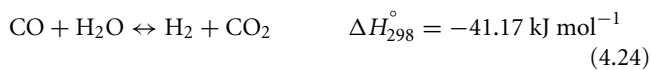
CO$_2$ (dry) REFORMING OF GLYCEROL

Natural gas obtained from shale gas technology is a non-renewable source of energy which requires energy intensive processing. Depletion in fossil fuels and natural gas reserves prompted researchers to find ways in utilizing renewable resources for reforming processes. In this aspect, biofuels like ethanol and biodiesel are gaining considerable significance (Wang et al., 2009).
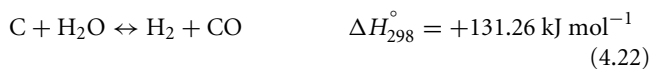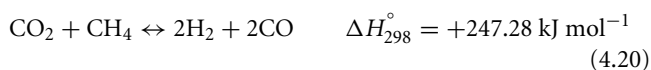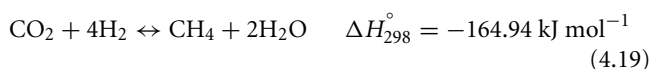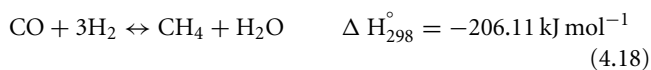
Glycerol, an oxygenated hydrocarbon, is a byproduct of the biodiesel production process by transesterification of vegetable oils and methanol (Wang et al., 2009). In recent years the process of producing hydrogen/syngas from glycerol reforming is becoming increasingly important due to the green chemical properties of glycerol such as non-toxic, non-volatile and non-flammable (Kale and Kulkarni, 2010). Most investigations are based on autothermal/steam reforming of glycerol (Zhang et al., 2007a; Adhikari et al., 2008; Valliyappan et al., 2008), however, in recent years, there is increasing research being carried out for dry reforming of glycerol (DRG). This is because steam reforming of glycerol results in significant H$_2$ production with high H$_2$/CO ratio, thus rendering the reaction products inappropriate for the downstream Fischer Tropsch synthesis for production of gasoline. As such, water/steam needs to be replaced with CO$_2$ in order to maintain the H$_2$/CO ratio <2 (Siew et al., 2014).

Furthermore, research on CO$_2$ DRE has shown that CO$_2$ can be sequestered and carbon deposits in the form of CNFs can be formed. These CNFs have commercial potential. Likewise glycerol dry reforming can also be expected to facilitate CNFs production

(Kale and Kulkarni, 2010). These high values inert carbon can result in removal of CO_2 from the carbon biosphere cycle (Wang et al., 2009).

According to Wang et al. (2009), the main reactions which may take place during DRG are as follows:

$$C_3H_8O_3 \leftrightarrow 4H_2 + 3CO \qquad \Delta H^{\circ}_{298} = +251.18 \text{ kJ mol}^{-1} \tag{4.17}$$

$$CO + 3H_2 \leftrightarrow CH_4 + H_2O \qquad \Delta H^{\circ}_{298} = -206.11 \text{ kJ mol}^{-1} \tag{4.18}$$

$$CO_2 + 4H_2 \leftrightarrow CH_4 + 2H_2O \qquad \Delta H^{\circ}_{298} = -164.94 \text{ kJ mol}^{-1} \tag{4.19}$$

$$CO_2 + CH_4 \leftrightarrow 2H_2 + 2CO \qquad \Delta H^{\circ}_{298} = +247.28 \text{ kJ mol}^{-1} \tag{4.20}$$

$$CO + H_2O \leftrightarrow H_2 + CO_2 \qquad \Delta H^{\circ}_{298} = -41.17 \text{ kJ mol}^{-1} \tag{4.21}$$

$$C + H_2O \leftrightarrow H_2 + CO \qquad \Delta H^{\circ}_{298} = +131.26 \text{ kJ mol}^{-1} \tag{4.22}$$

$$CH_4 \leftrightarrow 2H_2 + C \qquad \Delta H^{\circ}_{298} = +74.85 \text{ kJ mol}^{-1} \tag{4.23}$$

$$CO + H_2O \leftrightarrow H_2 + CO_2 \qquad \Delta H^{\circ}_{298} = -41.17 \text{ kJ mol}^{-1} \tag{4.24}$$

$$C + H_2O \leftrightarrow H_2 + CO \qquad \Delta H^{\circ}_{298} = +131.26 \text{ kJ mol}^{-1} \tag{4.25}$$

$$2CO \leftrightarrow CO_2 + C \qquad \Delta H^{\circ}_{298} = -172.43 \text{ kJ mol}^{-1} \tag{4.26}$$

$$C + 2H_2O \leftrightarrow 2H_2 + CO_2 \qquad \Delta H^{\circ}_{298} = +74.85 \text{ kJ mol}^{-1} \tag{4.27}$$

Based on the main reactions, we can see that the carbon producing reactions are mainly from methane decomposition (Eq. 4.23) and Boudouard reactions (Eq. 4.26). Thermodynamic analysis conducted by Wang et al. (2009) and Cheng et al. (2012) showed that temperatures between 800 and 1000 K at 1 atm pressure represent the best conditions for optimal DRG performance. Methane, an undesirable by product is produced via CO (Eq. 4.18) and CO_2 hydrogenation (Eq. 4.19). CO/CO_2 hydrogenation being exothermic can result in suppression of methane formation at higher temperatures, and this has been supported by thermodynamic analysis (Wang et al., 2009).

Catalyst selection for DRG

Similar to methane reforming reactions, Ni-based catalysts are preferred for glycerol reforming, albeit their propensity for carbon deposition. Early studies on steam reforming of glycerol focus on Ni supported on various oxide supports such as Al_2O_3, MgO, $MgAl_2O_4$, SiO_2, ZrO_2, and CeO_2 (Ebshish et al., 2012). In fact, Ni-based catalysts can easily cleave the bonds between O–H, –CH_2–, C–C and –CH_3–, thereby possessing high activity for hydrogenation and dehydrogenation (Lee et al., 2014). Siew et al. (2014) investigated the performance of Ni/Al_2O_3 catalysts doped with La for DRG reaction at 873 K. They found that only 3% La promotion was sufficient to reduce the carbon deposition by 20%.

This catalyst composition was also found to display good stability over a 72-h test run at 1023 K at a weight hourly space velocity of 3.6×10^{-4} ml g^{-1} h^{-1} STP (Siew et al., 2015). Kinetic studies showed that glycerol decomposition and glycerol dehydrogenation as the most probably competing route in a parallel pathway for syngas production. Methane was also produced as a byproduct from glycerol dehydrogenation. The authors proposed that CO_2 played a role in promoting RWGS reaction (Siew et al., 2014). In another recent study, Lee et al. (2014) investigated the use of cement clinker-supported Ni catalyst with various loadings for DRG reaction. Physicochemical analysis techniques revealed that cement clinker was a complex mixture of CaO (62%) and SiO (17%) oxide compounds. They found that Ni loadings of 20 wt% led to desirable syngas production with H_2/CO ratio of 1.5 and low methane selectivity at 1023 K (Lee et al., 2014).

FUTURE PERSPECTIVES

In terms of catalyst development, there still exists room for improvement in terms of catalyst development with superior catalytic activity, selectivity and stability (minimum carbon deposition), albeit at a low cost. This can be achieved via synthesis of embedded core–shell type catalysts. The encapsulation of active metal nanoparticles in the cavities of porous structures provides an alternative feasible route for the design of core–shell type catalysts owing to their large surface area making them ideal for catalysis, as well as energy storage and conversion applications (Zhang et al., 2013). As an example, Mo et al. (2014) developed the *in situ* self-assembled core–shell precursor route for synthesis of embedded core–shell catalysts having good dispersion, which is the essential factor in enhancing the catalytic activity and stability, by imparting anti-coking properties for the DRM reaction. This is a good progress in terms of industrial catalyst development. As such, fundamental studies, which can provide a clear insight in terms of molecular level understanding of the catalyst geometry and active sites, are one of the important aspects that need to be addressed. Indirectly, insights gained from the fundamental studies are correlated to the implications of cost involved in developing the catalyst, which is an important factor for process feasibility. The next factor, which requires much research, is on large-scale production of catalysts, especially nano-catalysts. Even though the catalyst synthesis may have been proven in lab scale, however, they require extensive fine-tuning for reproducibility and industrial scalability as well as the need for consideration of environmental factors involved during catalyst synthesis.

Another important limitation that needs to be addressed is in terms of the process energy requirements. The setting up of industrial processes utilizing CO_2 for reactions such as ODH and reforming is one of the long-term major goals of chemists and engineers alike, in view of the potential long-term global environmental benefits. In fact, the current gaps of knowledge stem from the reaction process energy and economic aspects. Hence, the possible solution for improving the energy aspect is via process intensification.

In fact, for steam reforming of methane, Sulzer has developed a combined static-mixer reactor consisting of heat transfer tubes as well as monolithic catalytic reactors placed within the piping (Stankiewicz and Moulijn, 2000). In another development,

micro-channel catalyst coated reactors have been developed by Velocys, also for steam reforming of methane. It was found that by employing such micro-channel reactors, considerable improvement in terms of contact time of reactor fluid with catalyst which results in 300-fold increase in production capacity/volume can be achieved (Tonkovich et al., 2007). These developments for the steam reforming of methane reactors are especially beneficial and applicable to dry reforming of hydrocarbons/alcohol, as the nature of both steam/CO_2-mediated reactions are endothermic. In this approach, noble metal catalysts are directly coated on the metal extended surfaces. This integration of heat transfer as well as catalytic dehydrogenation/reforming reaction can lead to supply of thermal energy to the catalysts at a rate adequate in maintaining high catalytic activity. Moreover, compared to traditional reformers, which require radiation of heat to tubes, followed by heat conduction through contact resistances to the catalysts (in pellet form) inside the tubes; the heat transfer ability in catalyzed heat exchangers can be tremendously improved (Valensa, 2009).

In terms of process design improvements especially for industrial generation of hydrogen, an emerging technology that has tremendous advantages to offer is the precious metal monolith catalyst for advancement of new steam reformer designs (Farrauto et al., 2007). The monoliths with "washcoats," which contain precious metals (where the precious metals are well dispersed on high surface area carriers such as thermally stabilized alumina) have excellent mechanical and chemical resistance, low pressure drop, and a more compact size compared to reactors with traditional pellets or particulate materials. The need for temperature control can be met by technological advancements in the form of catalyzed heat exchangers in the reformers. In fact, deposition of highly active noble metal catalyzed washcoat on the monolithic heat exchanger results in up to 10 times greater space velocity (reduction in reactor size) compared to traditional processes by eliminating heat transfer resistance, which govern pelletized packed bed reforming processes (Farrauto et al., 2007). For example, Polman et al. (1999) designed a steam reformer whereby the inner reactor contain a series of plates with a metal monolithic structure which alternate between corrugated foils and flat high-temperature steel. The monolith compartments were alternatively washcoated with combustion and steam reforming catalysts. The steam reforming compartments receive the heat generated from the combustion compartment via the steel plates.

On the other hand, in order to maintain thermoneutrality of the reaction, much research has been carried out to improve the process efficiency as well as economic viability of the reactions involving utilization of CO_2 as an oxidant or as a reforming agent. In order to achieve this, supply of oxygen provides exothermal energy, which can reduce the energy requirements (Jiang et al., 2011). However, conventional oxygen supply via the pressure swing adsorption (PSA) method requires high investment (Liang and Caro, 2011). Besides, supply of oxygen externally in the form of molecular oxygen, gives rise to combustion of hydrocarbons (especially at high quantities) and thus may not be particularly effective for improving selectivity.

One such solution to circumvent these issues is by providing oxygen supply *in situ* at controlled amounts. The catalytic membrane reactor configuration combines a perm-selective membrane for separation of oxygen from air which is to be supplied to the chemical process. Catalytic membrane reactors are the strategic means for process intensification and thus markedly improving the existing replace conventional packed bed reactor based processes (Fontananova and Drioli, 2010) for CO_2-mediated oxidative high-temperature reactions.

In terms of process, in order to enhance the conversion of CO_2-mediated ODH reactions, controlling the contact mode of oxygen to the reactants is important to improve selectivity toward olefin production (Wang et al., 2006). On the other hand, the combination of DRM with partial oxidation is beneficial in tailoring the syngas product ratio of H_2:CO to 1–2 for further downstream Fischer–Tropsch reactions.

In order to supply the required oxygen across the membrane, dense mixed ionic and electronic conducting perovskite-type membranes have much potential since external circuitry is not required (Caro et al., 2007). The ceramic oxygen permeable membranes are highly selective to O_2 and catalyze the dissociation of O_2 molecule into oxygen ions, O^{2-} which permeate across the membrane based on the O_2 partial pressure gradient (Smart et al., 2014). The membrane functions as a distributor of the oxygen, which in its ionic state promotes selectivity toward product formation. In other words, lattice oxygen supply from the mixed ionic and electronic conducting membranes inhibits combustion and the distributed mode of oxygen supply along the membrane channel further prevents formation of hot spots (Yang et al., 2013).

For example, for CO_2-oxidative coupling of methane reactions, a perovskite membrane which provides O^{2-} supply from air can selectively convert methane to C_2 products, thus avoiding gas phase reactions and deep combustion of methyl radicals. The products can be channeled to second-stage catalytic membrane reactor equipped with perm-selective membranes, which can remove H_2 from the product stream upon dehydrogenation. This inadvertently can lead to shift in equilibrium, thus allowing for higher product conversion toward more olefin production. This concept is a good platform for process intensification and overall improvements.

Despite the energy savings, environmental sustainability, compact unit operation, and improved catalytic performance associated with integrated catalytic membrane reactor concept for CO_2-mediated dehydrogenation/reforming reactions, there are however, some restrictions for industrial implementation. The main barrier lies in the fundamental issue pertaining to stability of the membrane in corrosive and reducing environment. Nevertheless, recent research developments show much focus on the design of chemically tolerant membranes. This is proven based on several successful studies on the implementation of integrated catalytic membrane reactor systems for reactions such as CO_2-mediated reforming of methane (Slade et al., 2007; Yang et al., 2013; Kathiraser et al., 2013b). Substantial work, however, is required to enhance the robustness as well as inherent permeability characteristics of the membrane under the harsh chemical reaction environment.

CONCLUSION

In recent years, the need to reduce escalating CO_2 emissions to the atmosphere has become increasingly important. One method

that can not only reduce CO_2 emission, but also can lead to production of valuable products is by utilizing CO_2 as an oxidant. Most of the reactions utilizing CO_2 for high-temperature applications relate to the role of CO_2 as an intermediary in saturated hydrocarbon conversion to olefins with release of hydrogen molecule. The nature and properties of the catalysts such as redox or acid–base play an important role in determining the catalytic activity as well as selectivity toward olefin production. Improvements in the yield of olefins production remain a key factor, which requires much on-going research. On the other hand, utilization of CO_2 for hydrocarbon reforming offer much potential for hydrogen/syngas production. Syngas is an important building block for chemical production. Much efforts are emphasized toward synthesis of active and stable catalysts for CO_2 reforming of methane (the simplest hydrocarbon molecule but requires greatest dissociation energy compared to other hydrocarbons). In this aspect, Ni is the most widely studied transition metal for reforming process in view of its wide availability and economic cost, compared to noble metals. Various improvements in catalyst structures have been made, with much effort directed toward synthesis of highly dispersed Ni nano-catalysts. However, besides methane, much research efforts have been targeted toward reforming of sustainable renewable sources such as ethanol and glycerol. Besides, syngas/hydrogen, reforming of these alcohols can be a potential source of CNFs, which have found a niche in the market. Utilizing renewable resources pave the way toward utilizing CO_2 in an environmentally sustainable manner in order to produce valuable energy/chemicals/products, which are much need in this global age.

ACKNOWLEDGMENTS

REFERENCES

Abatzoglou, N., Blanchard, J., Oudghiri-Hassani, H., Jankhah, S., and Gitzhofer, F. (2006). "The use of catalytic reforming reactions for CO_2 sequestration as carbon nanotubes," in *Proceedings of the 2006 IASME/WSEAS International Conference on Energy & Environmental Systems*, (Chalkida: World Scientific and Engineering Academy and Society), 21–26.

Adhikari, S., Fernando, S., To, S. D. F., Bricka, R. M., Steele, P. H., and Haryanto, A. (2008). Conversion of glycerol to hydrogen via a steam reforming process over nickel catalysts. *Energy Fuels* 22, 1220–1226. doi:10.1021/ef700520f

Al-Muhaish, F.I., Ahmed, S., Bittencourt, R.C.P., Cardoso, M.J.B., and Souza, D. V.P. (2015). *Catalyst and Process for Thermo-Neutral Reforming of Liquid Hydrocarbons*. US Patent Application US20150013225A1.

Ansari, M. A., and Park, S. E. (2012). Carbon dioxide utilization as a soft oxidant and promoter in catalysis. *Energy Environ. Sci.* 5, 9419–9437. doi:10.1039/c2ee22409g

Arena, F., Horrell, B. A., Cocke, D. L., Parmaliana, A., and Giordano, N. (1991). Magnesia-supported nickel catalysts I. Factors affecting the structure andmorphological properties. *J. Catal.* 132, 58–67. doi:10.1016/0021-9517(91)90246-Z

Aresta, M., Dibenedetto, A., and Angelini, A. (2013). The changing paradigm in CO_2 utilization. *J. CO_2 Util.* 3–4, 65–73. doi:10.1016/j.jcou.2013.08.001

Arnold, S.C., Koegler, J.H., Gaffney, A.M., Yeh, C.Y., and Song, R. (2014). *Combined Carbon Dioxide and Oxygen Process for Ethylbenzene Dehydrogenation to Styrene*. US Patent US8765082 B2.

Ba, H., Podila, S., Liu, Y., Mu, X., Nhut, J. M., Papaefthimiou, V., et al. (2014). Nanodiamond decorated few-layer graphene composite as an efficient metal-free dehydrogenation catalyst for styrene production. *Catal. Today* doi:10.1016/j.cattod.2014.10.029

Badstube, T., Papp, H., Kustrowski, P., and Dziembaj, R. (1998). Oxidative dehydrogenation of ethylbenzene with carbon dioxide on alkali-promoted Fe/active carbon catalysts. *Catal. Lett.* 55, 169–172. doi:10.1023/A:1019099332393

Baek, J., Yun, H. J., Yun, D., Choi, Y., and Yi, J. (2012). Preparation of highly dispersed chromium oxide catalysts supported on mesoporous silica for the oxidative dehydrogenation of propane using CO_2: insight into the nature of catalytically active chromium sites. *ACS Catal.* 2, 1893–1903. doi:10.1021/cs300198u

Bartholomew, C. H. (1984). Catalyst deactivation. *Chem. Eng.* 91, 96–112.

Batiot-Dupeyrat, C., Valderrama, G., Meneses, A., Martinez, F., Barrault, J., and Tatibouë, J. M. (2003). Pulse study of CO_2 reforming of methane over LaNiO$_3$. *Appl. Catal. A Gen.* 248, 143–151. doi:10.1016/S0926-860X(03)00155-8

Bellido, J. D. A., Tanabe, E. Y., and Assaf, E. M. (2009). Carbon dioxide reforming of ethanol over Ni/Y$_2$O$_3$-ZrO$_2$ catalysts. *Appl. Catal. B* 90, 485–488. doi:10.1016/j.apcatb.2009.04.009

Bhattacharyya, A., and Chang, V. W. (1994). CO_2 reforming of methane to syngas: deactivation behavior of nickel aluminate spinel catalysts. *Stud. Surf. Sci. Catal.* 88, 207–213. doi:10.1016/S0167-2991(08)62742-1

Bitter, J. H., Seshan, K., and Lercher, J. A. (1999). Deactivation and coke accumulation during CO_2/CH_4 reforming over Pt catalysts. *J. Catal.* 183, 336–343. doi:10.1006/jcat.1999.2402

Blanchard, J., Oudghiri-Hassani, H., Abatzoglou, N., Jankhah, S., and Gitzhofer, F. (2008). Synthesis of nanocarbons via ethanol dry reforming over a carbon steel catalyst. *Chem. Eng. J.* 143, 186–194. doi:10.1016/j.cej.2008.04.012

Blasco, T., Nieto, J. M. L., Dejoz, A., and Vazaquez, M. I. (1995). Influence of the acid-base character of supported vanadium catalysts on their catalytic properties for the oxidative dehydrogenation of *n*-butane. *J. Catal.* 157, 271–282. doi:10.1006/jcat.1995.1291

Botavina, M. A., Martra, G., Agafonov, Y. A., Gaidai, N. A., Nekrasov, N. V., Trushin, D. V., et al. (2008). Oxidative dehydrogenation of C$_3$–C$_4$ paraffins in the presence of CO_2 over CrO$_x$/SiO$_2$ catalysts. *Appl. Catal. A Gen.* 347, 126–132. doi:10.1016/j.apcata.2008.05.037

Bradford, M. C. J., and Vannice, M. A. (1999). CO_2 reforming of CH_4. *Catal. Rev. Sci. Eng.* 41, 1–42. doi:10.1081/CR-100101948

Budin, L.M., and Meyer, L.M. (2003). *Oxidative Dehydrogenation of Alkanes to Olefins Using an Oxide Surface*. US Patent Application WO2003011444 A2.

Burri, A., Jiang, N., Ji, M., Park, S. E., and Khalid, Y. (2013). Oxidative dehydrogenation of ethylbenzene to styrene with CO_2 over V$_2$O$_5$–Sb$_2$O$_5$–CeO$_2$/TiO$_2$–ZrO$_2$ catalysts. *Top. Catal.* 56, 1724–1730. doi:10.1007/s11244-013-0108-0

Burri, D. R., Choi, K. M., Han, S. C., Burri, A., and Park, S. E. (2007). Selective conversion of ethylbenzene into styrene over K$_2$O/TiO$_2$-ZrO$_2$ catalysts: unified effects of K$_2$O and CO_2. *J. Mol. Catal. A Chem.* 269, 58–63. doi:10.1016/j.molcata.2006.12.021

Carja, G., Nakamura, R., Aida, T., and Niiyama, H. (2003). Mg–V–Al mixed oxides with mesoporous properties using layered double hydroxides as precursors: catalytic behavior for the process of ethylbenzene dehydrogenation to styrene under a carbon dioxide flow. *J. Catal.* 218, 104–110. doi:10.1016/S0021-9517(03)00051-4

Caro, J., Caspary, K. J., Hamel, C., Hoting, B., Kolsch, P., Langanke, B., et al. (2007). Catalytic membrane reactors for partial oxidation using perovskite hollow fiber membranes and for partial hydrogenation using a catalytic membrane contactor. *Ind. Eng. Chem. Res.* 46, 2286–2294. doi:10.1021/ie0609620

Castro, A. J. R., Soares, J. M., Filho, J. M., Oliveira, A. C., Edwin, A. C., and Milet, R. C. (2013). Oxidative dehydrogenation of ethylbenzene with CO_2 for styrene production over porous iron-based catalysts. *Fuel* 108, 740–748. doi:10.1016/j.fuel.2013.02.019

Cavani, F., Koutyrev, M., Trifiro, F., Bartolini, A., Ghisletti, D., Iezzi, R., et al. (1996). Chemical and physical characterization of alumina-supported chromia-based catalysts and their activity in dehydrogenation of isobutene. *J. Catal.* 158, 236–250. doi:10.1006/jcat.1996.0023

Cheng, C. K., Foo, S. Y., and Adesina, A. A. (2012). Thermodynamic analysis of glycerol dry reforming in the presence of CO_2 or H_2 as carbon gasifying agent. *Int. J. Hydrogen Energy* 37, 10101–10110. doi:10.1016/j.biortech.2008.11.021

Corthals, S., Van Nederkassel, J., Geboers, J., De Winne, H., Van Noyen, J., Moens, B., et al. (2008). Influence of composition of MgAl$_2$O$_4$ supported NiCeO$_2$ZrO$_2$ catalysts on coke formation and catalyst stability for dry reforming of methane. *Catal. Today* 138, 28–32. doi:10.1016/j.cattod.2008.04.038

de Araujo, J. C. S., Souza, C. B. A., Oliveira, A. C., Freire, F. N. A., Ayala, A. P., and Oliveira, A. C. (2010). Dehydrogenation of ethylbenzene with CO_2 to produce styrene over Fe-containing ceramic composites. *Appl. Catal. A Gen.* 377, 55–63. doi:10.1016/j.apcata.2010.01.016

de Lima, S. M., da Cruz, I. O., Jacobs, G., Davis, B. H., Mattos, L. V., and Noronha, F. B. (2008). Steam reforming, partial oxidation, and oxidative steam reforming of ethanol over Pt/CeZrO₂ catalyst. *J. Catal.* 257, 356–368. doi:10.1016/j.jcat.2008.05.017

de Lima, S. M., da Silva, A. M., Jacobs, G., Davis, B. H., Mattosa, L. V., and Noronha, F. B. (2010). New approaches to improving catalyst stability over Pt/ceria during ethanol steam reforming: Sn addition and CO_2 co-feeding. *Appl. Catal. B* 96, 387–398. doi:10.1016/j.apcatb.2010.02.036

de Llobet, S., Pinilla, J. L., Moliner, R., and Suelves, I. (2015). Effect of the synthesis conditions of Ni/Al₂O₃ catalysts on the biogas decomposition to produce H₂-rich gas and carbon nanofibers. *Appl. Catal. B* 165, 457–465. doi:10.1016/j.apcatb.2014.10.014

Deng, S., Li, H., Li, S., and Zhang, Y. (2007). Activity and characterization of modified Cr₂O₃/ZrO₂ nano-composite catalysts for oxidative dehydrogenation of ethane to ethylene with CO_2. *J. Mol. Catal. A Chem.* 268, 169–175. doi:10.1016/j.molcata.2006.12.033

Dury, F., Gaigneaux, E. M., and Ruiz, P. (2003a). The active role of CO_2 at low temperature in oxidation processes: the case of the oxidative dehydrogenation of propane on NiMoO₄ catalysts. *Appl. Catal. A Gen.* 242, 187–203. doi:10.1016/S0926-860X(02)00516-1

Dury, F., Centeno, M. A., Gaigneaux, E. M., and Ruiz, P. (2003b). An attempt to explain the role of CO_2 and N₂O as gas dopes in the feed in the oxidative dehydrogenation of propane. *Catal. Today* 81, 95–105. doi:10.1016/S0920-5861(03)00120-2

Ebshish, A., Yaakob, Z., Taufiq-Yap, Y. H., Bshish, A., and Tasirin, S. M. (2012). Review of hydrogen production via glycerol reforming. *Proc I Mech E Part A J Power Energy* 226, 1060–1075. doi:10.1177/0957650912464624

Erdöhelyi, A., Cserényi, J., Papp, E., and Solymosi, F. (1994). Catalytic reaction of methane with carbon dioxide over supported palladium. *Appl. Catal. A Gen.* 108, 205–219. doi:10.1016/0926-860X(94)85071-2

Fan, M.-S., Abdullah, A. Z., and Bhatia, S. (2009). Catalytic technology for carbon dioxide reforming of methane to synthesis gas. *ChemCatChem* 1, 192–208. doi:10.1002/cctc.200900025

Farrauto, R. J., Liu, Y., Ruettinger, W., Ilinich, O., Shore, L., and Giroux, T. (2007). Precious metal catalysts supported on ceramic and metal monolithic structures for the hydrogen economy. *Catal. Rev.* 49, 141–196. doi:10.1080/01614940701220496

Fontananova, E., and Drioli, E. (2010). Catalytic membranes and membrane reactors. *Compr. Membr. Sci. Eng.* 3, 109–133. doi:10.1016/B978-0-08-093250-7.00022-0

Gallego, G. S., Mondrago, F., Barrault, J., Tatibouet, J. M., and Batiot-Dupeyrat, C. (2006). CO_2 reforming of CH₄ over La–Ni based perovskite precursors. *Appl. Catal. A Gen.* 311, 164–171. doi:10.1016/j.apcata.2006.06.024

Gallego, G. S., Mondragón, F., Tatibouët, J. M., Barrault, J., and Batiot-Dupeyrat, C. (2008). Carbon dioxide reforming of methane over La₂NiO₄ as catalyst precursor—Characterization of carbon deposition. *Catal. Today* 13, 200–209. doi:10.1016/j.cattod.2007.12.075

Gao, J., Hou, Z., Lou, H., and Zheng, X. (2011). "Dry (CO_2) reforming, Chapter 7," in *Fuel Cells: Technologies for fuel processing*, eds D. Shekhawat, J. J. Spivey, and D. A. Berry (Oxford: Elsevier B. V.), 191–221. doi:10.1016/B978-0-444-53563-4.10007-0

Gaur, S., Pakhare, D., Wu, H., Haynes, D. J., and Spivey, J. J. (2012). CO_2 reforming of CH₄ over Ru-substituted pyrochlore catalysts: effects of temperature and reactant feed ratio. *Energy Fuels* 26, 1989–1998. doi:10.1021/ef300158y

Ge, S., Liu, C., Zhang, S., and Li, Z. (2003). Effect of carbon dioxide on the reaction performance of oxidative dehydrogenation of *n*-butane over V-Mg-O catalyst. *Chem. Eng. J.* 94, 121–126. doi:10.1016/S1385-8947(03)00023-8

Han, S., Jin, L., Martenak, D.J., and Suib, S.L. (2010). *Improved Process for the Oxidative Dehydrogenation of Ethane*. European Patent Application EP2165997 A1.

Hu, X., and Lu, G. (2009). Syngas production by CO_2 reforming of ethanol over Ni/Al₂O₃ catalyst. *Catal. Commun.* 10, 1633–1637. doi:10.1016/j.catcom.2009.04.030

Irún, O., Sadosche, S. A., Lasobras, J., Soler, J., Francés, E., Herguido, J., et al. (2013). Catalysts for the production of styrene from ethylbenzene: redox and deactivation study. *Catal. Today* 203, 53–59. doi:10.1016/j.cattod.2012.07.019

Jankhah, S., Abatzoglou, N., and Gitzhofer, F. (2008). Thermal and catalytic dry reforming and cracking of ethanol for hydrogen and carbon nanofilaments' production. *Int. J. Hydrogen Energy* 33, 4769–4779. doi:10.1016/j.ijhydene.2008.06.058

Jiang, N., Han, D. S., and Park, S. E. (2009). Direct synthesis of mesoporous silicalite-1 supported TiO₂–ZrO₂ for the dehydrogenation of EB to styrene with CO_2. *Catal. Today* 141, 344–348. doi:10.1016/j.cattod.2008.04.033

Jiang, Q., Faraji, S., Slade, D. A., and Stagg-Williams, S. M. (2011). Chapter 11- A review of mixed ionic and electronic conducting ceramic membranes as oxygen sources for high temperature reactions. *Membr. Sci. Technol.* 14, 235–273. doi:10.1016/B978-0-444-53728-7.00011-2

Jimenez-Gonzalez, C., Boukha, Z., de Rivas, B., Gonzalez-Velasco, J. R., Gutierrez-Ortiz, J. I., and Lopez-Fonseca, R. (2015). Behaviour of nickel-alumina spinel (NiAl₂O₄) catalysts for isooctane steam reforming. *Int. J. Hydrogen Energy* doi:10.1016/j.ijhydene.2015.01.064

Kale, G. R., and Kulkarni, B. D. (2010). Thermodynamic analysis of dry autothermal reforming of glycerol. *Fuel Process. Technol.* 91, 520–530. doi:10.1016/j.fuproc.2009.12.015

Kathiraser, Y., Thitsartarn, W., Sutthiumporn, K., and Kawi, S. (2013a). Inverse NiAl₂O₄ on LaAlO₃–Al₂O₃: unique catalytic structure for stable CO_2 reforming of methane. *J. Phys. Chem. C* 117, 8120–8130. doi:10.1021/jp401855x

Kathiraser, Y., Wang, Z., and Kawi, S. (2013b). Oxidative CO_2 reforming of methane in La₀.₆Sr₀.₄Co₀.₈Ga₀.₂O₃₋δ (LSCG) hollow fiber membrane. *Environ. Sci. Technol.* 47, 14510–14517. doi:10.1021/es403158k

Khavarian, M., Chai, S. P., and Mohamed, A. R. (2014). Direct use of as-synthesized multi-walled carbon nanotubes for carbon dioxide reforming of methane for producing synthesis gas. *Chem. Eng. J.* 257, 200–208. doi:10.1016/j.cej.2014.05.079

Lee, D. W., Yu, C. Y., and Lee, K. H. (2008). Study on hydrothermal stability and catalytic activity of nanosphere-walled mesoporous silica. *J. Phys. Chem. C* 112, 5136–5140. doi:10.1021/jp712051p

Lee, H. C., Siew, K. W., Khan, M. R., Chin, S. Y., Gimbun, J., and Cheng, C. K. (2014). Catalytic performance of cement clinker supported nickel catalyst in glycerol dry reforming. *J. Energy Chem.* 23, 645–656. doi:10.1016/S2095-4956(14)60196-0

Lezla, O., Bordes, E., Courtine, P., and Hecquet, G. (1997). Synergetic effects in the Ni-Mo-O system: influence of preparation on catalytic performance in the oxidative dehydrogenation of propane. *J. Catal.* 170, 346–356. doi:10.1006/jcat.1997.1759

Li, W., Li, X., and Feng, J. (2009). Behaviors of V-doped titanium mixed oxides in the catalytic dehydrogenation of ethylbenzene. *Catal. Lett.* 130, 575–582. doi:10.1007/s10562-009-9971-5

Li, Z., Mo, L., Kathiraser, Y., and Kawi, S. (2014a). Yolk–satellite–shell structured Ni–Yolk@Ni@SiO₂nanocomposite: superb catalyst toward methane CO_2 reforming reaction. *ACS Catal.* 4, 1526–1536. doi:10.1021/cs401027p

Li, Z., Kathiraser, Y., and Kawi, S. (2014b). Facile synthesis of high surface area yolk–shell Ni@Ni embedded SiO₂ via Ni phyllosilicate with enhanced performance for CO_2 reforming of CH₄. *ChemCatChem* 7, 160–168. doi:10.1002/cctc.201402673

Li, Z., Kathiraser, Y., Ashok, J., Oemar, U., and Kawi, S. (2014c). Simultaneous Tuning Porosity and Basicity of Nickel@Nickel–Magnesium Phyllosilicate Core–Shell Catalysts for CO_2 Reforming of CH₄. *Langmuir* 30, 14694–14705. doi:10.1021/la503340s

Liang, F., and Caro, J. (2011). "Perovskite membranes for high temperature oxygen separation," in *Membrane Engineering for the Treatment of Gases, Volume 2: Gas-Separation Problems Combined with Membrane Reactors*, eds E. Drioli and G. Barbieri (Cambridge, UK: Royal Society of Chemistry), 192–221.

Liu, H., Zhang, Z., Li, H., and Huang, Q. (2011). Intrinsic kinetics of oxidative dehydrogenation of propane in the presence of CO_2 over Cr/MSU-1 catalyst. *J. Nat. Gas Chem.* 20, 311–317. doi:10.1016/S1003-9953(10)60180-6

Liu, L., and Li, H. (2006). A comparative study on catalytic performances of chromium incorporated and supported mesoporous MSU-x catalysts for the oxidehydrogenation of ethane to ethylene with carbon dioxide. *Catal. Today* 115, 235–241. doi:10.1016/j.cattod.2006.02.040

Liu, L., Li, H., and Zhang, Y. (2007). Mesoporous silica-supported chromium catalyst: characterization and excellent performance in dehydrogenation of propane to propylene with carbon dioxide. *Catal. Commun.* 8, 565–570. doi:10.1016/j.catcom.2006.08.005

Liu, Y. M., Cao, Y., Yi, N., Feng, W. L., Dai, W. L., Yan, S. R., et al. (2004). Vanadium oxide supported on mesoporous SBA-15 as highly selective catalysts in the

oxidative dehydrogenation of propane. *J. Catal.* 224, 417–428. doi:10.1016/j.jcat.2004.03.010

Mark, M. F., and Maier, W. F. (1996). CO$_2$-reforming of methane on supported Rh and Ir catalysts. *J. Catal.* 164, 122–130. doi:10.1006/jcat.1996.0368

McCoy, S. T., and Rubin, E. S. (2008). An engineering-economic model of pipeline transport of CO$_2$ with application to carbon capture and storage. *Int. J. Greenhouse Gas Control* 2, 219–229. doi:10.1016/S1750-5836(07)00119-3

Michorczyk, P., Pietrzyk, P., and Ogonowski, J. (2012). Preparation and characterization of SBA-1–supported chromium oxide catalysts for CO$_2$ assisted dehydrogenation of propane. *Microporous Mesoporous Mater.* 161, 56–66. doi:10.1016/j.micromeso.2012.05.011

Mimura, N., Okamoto, M., Yamashita, H., Oyama, S. T., and Murata, K. (2006). Oxidative dehydrogenation of ethane over Cr/ZSM-5 catalysts using CO$_2$ as an oxidant. *J. Phys. Chem. B* 110, 21764–21770. doi:10.1021/jp061966l

Mimura, N., and Saito, M. (2000). Dehydrogenation of ethylbenzene to styrene over Fe$_2$O$_3$/Al$_2$O$_3$ catalysts in the presence of carbon dioxide. *Catal. Today* 55, 173–178. doi:10.1016/S0920-5861(99)00236-9

Mo, L., Leong, K. K. M., and Kawi, S. (2014). A highly dispersed and anti-coking Ni–La$_2$O$_3$/SiO$_2$ catalyst for syngas production from dry carbon dioxide reforming of methane. *Catal. Sci. Technol.* 4, 2107–2114. doi:10.1039/c3cy00869j

Moradi, G. R., Rahmanzadeh, M., and Khosravian, F. (2014). The effects of partial substitution of Ni by Zn in LaNiO$_3$ perovskite catalyst for methane dry reforming. *J. CO$_2$ Util.* 6, 7–11. doi:10.1016/j.jcou.2014.02.001

Nagaoka, K., Seshan, K., Aika, K., and Lercher, J. A. (2001). Carbon deposition during carbon dioxide reforming of methane—comparison between Pt/Al$_2$O$_3$ and Pt/ZrO$_2$. *J. Catal.* 197, 34–42. doi:10.1006/jcat.2000.3062

Nakagawa, K., Kajita, C., Ikenaga, N. O., Gamo, M. N., Ando, T., and Suzuki, T. (2003). Dehydrogenation of light alkanes over oxidized diamond-supported catalysts in the presence of carbon dioxide. *Catal. Today* 84, 149–157. doi:10.1016/S0920-5861(03)00268-2

Ni, J., Chen, L., Lin, J., and Kawi, S. (2012). Carbon deposition on borated alumina supported nano-sized Ni catalysts for dry reforming of CH$_4$. *Nano Energy* 1, 674–686. doi:10.1016/j.nanoen.2012.07.011

Ni, J., Chen, L., Lin, J., Schreyer, M. K., Wang, Z., and Kawi, S. (2013). High performance of MgeLa mixed oxides supported Ni catalysts for dry reforming of methane: the effect of crystal structure. *Int. J. Hydrogen Energy* 38, 13631–13642. doi:10.1016/j.ijhydene.2013.08.041

Obradovic, A., Likozar, B., and Levec, J. (2013). Catalytic surface development of novel nickel plate catalyst with combined thermally annealed platinum and alumina coatings for steam methane reforming. *Int. J. Hydrogen Energy.* 38, 1419–1429. doi:10.1016/j.ijhydene.2012.11.015

Oemar, U., Hidajat, K., and Kawi, S. (2011). Role of catalyst support over PdO–NiO catalysts on catalyst activity and stability for oxy-CO$_2$ reforming of methane. *Appl. Catal. A Gen.* 402, 176–187. doi:10.1016/j.apcata.2011.06.002

Olah, G.A., and Prakash, G.K.S. (2013). *Conversion of Carbon Dioxide to Methanol Using Bi-Reforming of Methane or Natural Gas.* US Patent US8440729 B2.

Oliveira-Vigier, K. D., Abatzoglou, N., and Gitzhofer, F. (2005). Dry-reforming of ethanol in the presence of a 316 stainless steel catalyst. *Can. J. Chem. Eng.* 83, 978–984. doi:10.1002/cjce.5450830607

Pak, S., Qiu, P., and Lunsford, J. H. (1998). Elementary reactions in the oxidative coupling of methane over Mn/Na$_2$WO$_4$/SiO$_2$ and Mn/Na$_2$WO$_4$/MgO catalysts. *J. Catal.* 179, 222–230. doi:10.1006/jcat.1998.2228

Pakhare, D., Schwartz, V., Abdelsayed, V., Haynes, D., Shekhawat, D., Poston, J., et al. (2014). Kinetic and mechanistic study of dry (CO$_2$) reforming of methane over Rh-substituted La$_2$Zr$_2$O$_7$ pyrochlores. *J. Catal.* 316, 78–92. doi:10.1016/j.jcat.2014.04.023

Pakhare, D., Shaw, C., Haynes, D., Shekhawat, D., and Spivey, J. (2013a). Effect of reaction temperature on activity of Pt- and Ru-substituted lanthanum zirconate pyrochlores (La$_2$Zr$_2$O$_7$) for dry (CO$_2$) reforming of methane (DRM). *J. CO$_2$ Util.* 1, 37–42. doi:10.1016/j.jcou.2013.04.001

Pakhare, D., Wu, H., Narendra, S., Abdelsayed, V., Haynes, D., Shekhawat, D., et al. (2013b). Characterization and activity study of the Rh-substituted pyrochlores for CO$_2$(dry) reforming of CH$_4$. *Appl. Petrochem. Res.* 3, 117–129. doi:10.1007/s13203-013-0042-x

Pan, Y. X., Kuai, P., Liu, Y., Ge, Q., and Liu, C. J. (2010). Promotion effects of Ga$_2$O$_3$ on CO$_2$ adsorption and conversion over a SiO$_2$-supported Ni catalyst. *Energy Environ. Sci.* 3, 1322–1325. doi:10.1039/c0ee00149j

Park, S. E., and Ansari, M. B. (2013). "Carbon dioxide as soft oxidant and promoter in oxidation catalysis," in *New and Future Developments in Catalysis*, ed. S. L. Suib (Oxford, UK: Elsevier), 481–499. doi:10.1016/B978-0-444-53882-6.00017-6

Park, S.E., Chang, J.S., and Park, M.S. (2005). *Method for Catalytic Dehydrogenation of Hydrocarbons using Carbon Dioxide as a Soft Oxidant.* US Patent 6958427 B2.

Pena, M. A., and Fierro, J. L. G. (2001). Chemical structures and performance of perovskite oxides. *Chem. Rev.* 101, 1981–2018. doi:10.1021/cr980129f

Polman, E. A., Der Kinderen, J. M., and Thuis, F. M. A. (1999). Novel compact steam reformer for fuel cells with heat generation by catalytic combustion augmented by induction heating. *Catal. Today* 47, 347–351. doi:10.1016/S0920-5861(98)00316-2

Postole, G., Chowdhury, B., Pinki, K., Banerji, J., and Auroux, A. (2010). Knoevenagel condensation reaction over acid–base bifunctional nanocrystalline Ce$_x$Zr$_{1-x}$O$_2$ solid solutions. *J. Catal.* 269, 110–121. doi:10.1016/j.jcat.2009.10.022

Pramod, C. V., Raghavendra, C., Reddy, K. H. P., Babu, G. V. R., Rao, K. S. R., and Raju, B. D. (2014). Concept and progress in coupling of dehydrogenation and hydrogenation reactions through catalysts. *J. Chem. Sci.* 126, 311–317. doi:10.1007/s12039-014-0576-1

Puolakka, K. J., and Krause, A. O. I. (2007). Combined CO$_2$ reforming and partial oxidation of fuel compounds. *Catal. Lett.* 116, 87–93. doi:10.1007/s10562-007-9112-y

Qiao, A., Kalevaru, V. N., Radnik, J., Düvel, A., Heitjans, P., Hari Kumar, A. S., et al. (2014). Oxidative dehydrogenation of ethane to ethylene over V$_2$O$_5$/Al$_2$O$_3$ catalysts: effect of source of alumina on the catalytic performance. *Ind. Eng. Chem. Res.* 53, 18711–18721. doi:10.1021/ie5008344

Qiao, Y., Miao, C., Yue, Y., Xie, Z., Yang, W., Hua, W., et al. (2009). Vanadium oxide supported on mesoporous MCM-41 as new catalysts for dehydrogenation of ethylbenzene with CO$_2$. *Microporous Mesoporous Mater.* 119, 150–157. doi:10.1016/j.micromeso.2008.10.010

Raju, G., Reddy, B. M., Abhishek, B., Mo, Y. H., and Park, S. E. (2012). Synthesis of C4 olefins from n-butane over a novel VO$_x$/SnO$_2$–ZrO$_2$ catalyst using CO$_2$ as soft oxidant. *Appl. Catal. A Gen.* 423–424. doi:10.1016/j.apcata.2012.02.040

Raju, G., Reddy, B. M., and Park, S. E. (2014). CO$_2$ promoted oxidative dehydrogenation of *n*-butane over VO$_x$/MO$_2$–ZrO$_2$ (M Ce or Ti) catalysts. *J. CO$_2$ Util.* 5, 41–46. doi:10.1016/j.jcou.2013.12.003

Rangel, M. D. C., Monteiro, A. P. D. M., Oportus, M., Reyes, P., RAMOS, M. D. S., and Lima, S. B. (2012). "Ethylbenzene dehydrogenation in the presence of carbon dioxide over metal oxides," in *Greenhouse Gases-Capturing, Utilization and Reduction*, ed. G. Liu (Rijeka: INTECH Open Access Publisher), 117–136.

Rao, K. N., Reddy, B. M., Abishek, B., Seo, Y. H., Jiang, N., and Park, S. E. (2009). Effect of ceria on the structure and catalytic activity of V$_2$O$_5$/TiO$_2$–ZrO$_2$ for oxidehydrogenation of ethylbenzene to styrene utilizing CO$_2$ as soft oxidant. *Appl. Catal. B* 91, 649–656. doi:10.1016/j.apcatb.2009.07.003

Reddy, B. M., Jin, H., Han, D. S., and Park, S. E. (2008). Oxidative dehydrogenation of ethylbenzene to styrene with carbon dioxide over Fe$_2$O$_3$/TiO$_2$–ZrO$_2$ catalyst: influence of chloride. *Catal. Lett.* 124, 357–363. doi:10.1007/s10562-008-9475-8

Reddy, G. K., Boolchand, P., and Smirniotis, P. G. (2012). Unexpected behavior of copper in modified ferrites during high temperature WGS reaction-aspects of Fe^{3+} ↔ Fe^{2+} redox chemistry from Mössbauer and XPS studies. *J. Phys. Chem. C* 116, 11019–11031. doi:10.1021/jp301090d

Rezaei, M., Alavi, S. M., Sahebdelfar, S., and Yan, Z. F. (2006). Syngas production by methane reforming with carbon dioxide on noble metal catalysts. *J. Nat. Gas Chem.* 15, 327–334. doi:10.1016/S1003-9953(07)60014-0

Rostrup-Nielsen, J. R., Sehested, J., and Norskov, J. K. (2002). Hydrogen and synthesis gas by steam- and CO$_2$ reforming. *Adv. Catal.* 47, 65–139. doi:10.1016/S0360-0564(02)47006-X

Ruckenstein, E., and Hu, Y. H. (1996). Role of support in CO$_2$ reforming of CH$_4$ to syngas over Ni catalysts. *J. Catal.* 162, 230–238. doi:10.1006/jcat.1996.0280

Sankar, M., Dimitratos, N., Miedziak, P. J., Wells, P. P., Kiely, C. J., and Hutchings, G. J. (2012). Designing bimetallic catalysts for a green and sustainable future. *Chem. Soc. Rev.* 41, 8099–8139. doi:10.1039/c2cs35296f

Sattler, J. J. H. B., Ruiz-Martinez, J., Santillan-Jimenez, E., and Weckhuysen, B. M. (2014). Catalytic dehydrogenation of light alkanes on metals and metal oxides. *Chem. Rev.* 114, 10613–10653. doi:10.1021/cr5002436

Schwint, K.J., and Wilcox, R.J. (2009). *Styrene Monomer Process Based on Oxidative Dehydrogenation of Ethylbenzene Using CO$_2$ as a Soft Oxidant.* Patent Application CA2723873A1.

Siew, K. W., Lee, H. C., Gimbun, J., and Cheng, C. K. (2014). Production of CO-rich hydrogen gas from glycerol dry reforming over La-promoted Ni/Al_2O_3 catalyst. *Int. J. Hydrogen Energy* 39, 6927–6936. doi:10.1016/j.ijhydene.2014.02.059

Siew, K. W., Lee, H. C., Gimbun, J., Chin, S. Y., Khan, M. R., Taufiq-Yap, Y. H., et al. (2015). Syngas production from glycerol-dry(CO_2) reforming over La-promoted Ni/Al_2O_3 catalyst. *Renew. Energy* 74, 441–447. doi:10.1016/j.renene.2014.08.048

Slade, D. A., Duncan, A. M., Nordheden, K. J., and Stagg-Williams, S. M. (2007). Mixed-conducting oxygen permeable ceramic membranes for the carbon dioxide reforming of methane. *Green Chem.* 9, 577–581. doi:10.1039/b614232j

Smart, S., Liu, S., Serra, J. M., Basile, A., and da Costa, J. C. D. (2014). "Perovskite membrane reactors: fundamentals and applications for oxygen production, syngas production and hydrogen processing," in *Membranes for Clean and Renewable Power Applications*, eds A. Gugliuzza and A. Basile (Cambridge: Woodhead Publishing Limited), 182–217.

Smith, R. S. (2008). *Simultaneous Dehydrogenation of Ethylbenzene and Ethane in the Presence of CO2 or Steam*. Patent Application CA2561986 A1.

Solsona, B., Blasco, T., Nieto, J. M. L., Peña, M. L., Rey, F., and Vidal-Moya, A. (2001). Vanadium oxide supported on mesoporous MCM-41 as selective catalysts in the oxidative dehydrogenation of alkanes. *J. Catal.* 203, 443–452. doi:10.1006/jcat.2001.3326

Solymosi, F., and Nemeth, R. (1999). The oxidative dehydrogenation of ethane with CO_2 over Mo_2C/SiO_2 catalyst. *Catal. Lett.* 62, 197–200. doi:10.1023/A:1019027912597

Solymosi, F., Nemeth, R., and Oszko, A. (2001). The oxidative dehydrogenation of propane with CO_2 over supported Mo_2C catalyst. *Stud. Surf. Sci. Catal.* 136, 339–344. doi:10.1016/S0167-2991(01)80326-8

Souza, M. M. V. M., Aranda, D. A. G., and Schmal, M. (2001). Reforming of methane with carbon dioxide over $Pt/ZrO_2/Al_2O_3$ catalysts. *J. Catal.* 204, 498–511. doi:10.1006/jcat.2001.3398

Souza, M. M. V. M., Aranda, D. A. G., and Schmal, M. (2002). Coke formation on $Pt/ZrO_2/Al_2O_3$ catalysts during CH_4 reforming with CO_2. *Ind. Eng. Chem. Res.* 41, 4681–4685. doi:10.1021/ie010970a

Stankiewicz, A. I., and Moulijn, J. A. (2000). Process intensification: transforming chemical engineering. *Chem. Eng. Prog.* 96, 22–34.

Styring, P., and Armstrong, K. (2011). Catalytic carbon dioxide conversions to value added chemicals. *Chimica Oggi Chem. Today* 29, 34–37.

Sutthiumporn, K., and Kawi, S. (2011). Promotional effect of alkaline earth over Ni–La_2O_3 catalyst for CO_2 reforming of CH_4: role of surface oxygen species on H_2 production and carbon suppression. *Int. J. Hydrogen Energy* 36, 14435–14446. doi:10.1016/j.ijhydene.2011.08.022

Sutthiumporn, K., Maneerung, T., Kathiraser, Y., and Kawi, S. (2012). CO_2 dry reforming of methane over $La_{0.8}Sr_{0.2}Ni_{0.8}M_{0.2}O_3$ perovskite (M Bi, Co, Cr, Cu, Fe): roles of lattice oxygen on C–H activation and carbon suppression. *Int. J. Hydrogen Energy* 37, 11195–11207. doi:10.1016/j.ijhydene.2012.04.059

Takehira, K., Ohishi, Y., Shishido, T., Kawabata, T., Takaki, K., Zhang, Q., et al. (2004). Behavior of active sites on Cr-MCM-41 catalysts during the dehydrogenation of propane with CO_2. *J. Catal.* 224, 404–416. doi:10.1016/j.jcat.2004.03.014

Tonkovich, A. L. Y., Yang, B., Perry, S., Fitzgerald, S. P., and Wang, Y. (2007). From seconds to milliseconds to microseconds through tailored microchannel reactor designs of a steam methane reformer. *Catal. Today* 120, 21–29. doi:10.1016/j.cattod.2006.07.022

Tsiakarasa, P., and Demin, A. (2001). Thermodynamic analysis of a solid oxide fuel cell system fuelled by ethanol. *J. Power Sources* 102, 210–217. doi:10.1016/S0378-7753(01)00803-5

Urlan, F., Marcu, I. C., and Sandulescu, I. (2008). Oxidative dehydrogenation of *n*-butane over titanium pyrophosphate catalysts in the presence of carbon dioxide. *Catal. Commun.* 9, 2403–2406. doi:10.1016/j.catcom.2008.05.038

Valderrama, G., Kiennemann, A., and Goldwasser, M. R. (2010). La-Sr-Ni-Co-O based perovskite-type solid solutions as catalyst precursors in the CO_2 reforming of methane. *J. Power Sources* 195, 1765–1771. doi:10.1016/j.jpowsour.2009.10.004

Valensa, J. (2009). *A Mixed-Dimensionality Modeling Approach for Interaction of Heterogeneous Steam Reforming Reactions and Heat Transfer*. Masters Theses, Marquette University, Milwaukee, WI.

Valliyappan, T., Bakhshi, N. N., and Dalai, A. K. (2008). Pyrolysis of glycerol for the production of hydrogen or syngas. *Bioresour. Technol.* 99, 4476–4483. doi:10.1016/j.biortech.2007.08.069

Van, D. B. P. J., Kramer, G. J., Murphy, A., and Vos, E. J. (2006). *Process for Steam and/or CO2 Reforming of a Hydrocarbonaceous Feedstock*. European Patent Application WO2006045744 A1.

Vasant, R. C., and Kartick, C. M. (2006). CO_2 reforming of methane combined with steam reforming or partial oxidation of methane to syngas over $NdCoO_3$ perovskite-type mixed metal-oxide catalyst. *Appl. Energy* 83, 1024–1032. doi:10.1016/j.apenergy.2005.09.008

Vilarrasa, V., Silva, O., Carrera, J., and Olivella, S. (2013). Liquid CO_2 injection for geological storage in deep saline aquifers. *Int. J. Greenhouse Gas Control.* 14, 84–96. doi:10.1016/j.ijggc.2013.01.015

Wang, H., Tablet, C., Schiestel, T., and Caro, J. (2006). Hollow fiber membrane reactors for the oxidative activation of ethane. *Catal. Today* 118, 98–103. doi:10.1016/j.cattod.2005.11.093

Wang, H., Zhang, J., and Dalai, A. K. (2011). *Catalyst for Production of Synthesis Gas*. US Patent US7985710 B2.

Wang, Q., Li, X., Li, W., and Feng, J. (2014a). Promoting effect of Fe in oxidative dehydrogenation of ethylbenzene to styrene with CO_2 (I) preparation and performance of $Ce_{1-x}Fe_xO_2$ catalyst. *Catal. Commun.* 50, 21–24. doi:10.1016/j.catcom.2014.02.014

Wang, Z., Cao, X. M., Zhu, J., and Hu, P. (2014b). Activity and coke formation of nickel and nickel carbide in dry reforming: a deactivation scheme from density functional theory. *J. Catal.* 311, 469–480. doi:10.1016/j.jcat.2013.12.015

Wang, W. (2011). Hydrogen production via dry reforming of butanol: thermodynamic analysis. *Fuel* 90, 1681–1688. doi:10.1016/j.fuel.2010.11.001

Wang, X., Li, M., Wang, M., Wang, S., Li, S., Wang, S., et al. (2009). Thermodynamic analysis of glycerol dry reforming for hydrogen and synthesis gas production. *Fuel* 88, 2148–2153. doi:10.1016/j.fuel.2009.01.015

Wu, X., and Kawi, S. (2009). Active and stable catalyst for CO_2 reforming of ethanol to hydrogen. *Catal. Today* 148, 251–259. doi:10.1016/j.cattod.2009.08.006

Yang, N. T., Kathiraser, Y., and Kawi, S. (2013). $La_{0.6}Sr_{0.4}Co_{0.8}Ni_{0.2}O_{3-\delta}$ hollow fiber membrane reactor: integrated oxygen separation–CO_2 reforming of methane reaction for hydrogen production. *Int. J. Hydrogen Energy.* 38, 4483–4491. doi:10.1016/j.ijhydene.2013.01.073

Yokota, S., Okumura, K., and Niwa, M. (2002). Support effect of metal oxide on Rh catalysts in the CH_4-CO_2 reforming reaction. *Catal. Lett.* 84, 131–134. doi:10.1023/A:1021097206196

Zawadzki, A., Bellido, J. D. A., Lucrédio, A. F., and Assaf, E. M. (2014). Dry reforming of ethanol over supported Ni catalysts prepared by impregnation with methanolic solution. *Fuel Process. Technol.* 128, 432–440. doi:10.1016/j.fuproc.2014.08.006

Zhang, B. C., Tang, X. L., Li, Y., Xu, Y., and Shen, W. J. (2007a). Hydrogen production from steam reforming of ethanol and glycerol over ceria-supported metal catalysts. *Int. J. Hydrogen Energy* 32, 2367–2373. doi:10.1016/j.ijhydene.2006.11.003

Zhang, J., Wang, H., and Dalai, A. K. (2007b). Development of stable bimetallic catalysts for carbon dioxide reforming of methane. *J. Catal.* 249, 300–310. doi:10.1016/j.jcat.2007.05.004

Zhang, J., Wang, H., and Dalai, A. K. (2008). Effects of metal content on activity and stability of Ni-Co bimetallic catalysts for CO_2 reforming of CH_4. *Appl. Catal. A Gen.* 339, 121–129. doi:10.1016/j.apcata.2008.01.027

Zhang, Q., Uchaker, E., Candelariaz, S. L., and Cao, G. (2013). Nanomaterials for energy conversion and storage. *Chem. Soc. Rev.* 42, 3128–3171. doi:10.1039/c3cs00009e

Zhang, X., Yue, Y., and Gao, Z. (2002). Chromium oxide supported on mesoporous SBA-15 as propane dehydrogenation and oxidative dehydrogenation catalysts. *Catal. Lett.* 83, 19–25. doi:10.1023/A:1021069510797

Zhang, Z. L., Tsipouriari, V. A., Efstathiou, A. M., and Verykios, X. E. (1996). Reforming of methane with carbon dioxide to synthesis gas over supported rhodium catalysts: I. Effects of support and metal crystallite size on reaction activity and deactivation characteristics. *J. Catal.* 158, 51–63. doi:10.1006/jcat.1996.0005

Zhao, S., and Wagner, J. P. (2004). *Nickel-Catalyst for Syngas Generation by Mixed Reforming Using CO2 and Steam*. US Patent Application WO2004011138 A1.

Zhao, X., and Wang, X. (2006). Oxidative dehydrogenation of ethane to ethylene by carbon dioxide over Cr/TS-1 catalysts. *Catal. Commun.* 7, 633–638. doi:10.1016/j.catcom.2006.02.005

Zhu, X., Huo, P., Zhang, Y., Cheng, D., and Liu, C. (2008). Structure and reactivity of plasma treated Ni/Al$_2$O$_3$ catalyst for CO$_2$ reforming of methane. *Appl. Catal. B* 81, 132–140. doi:10.1016/j.apcatb.2007.11.042

Conflict of Interest Statement: The authors declare that the research was conducted in the absence of any commercial or financial relationships that could be construed as a potential conflict of interest.